Chapter 9
Metal-Containing Nano-Antimicrobials: Differentiating the Impact of Solubilized Metals and Particles

Angela Ivask, Saji George, Olesja Bondarenko, and Anne Kahru

9.1 Metal-Containing Antimicrobials: Past, Current and Future

Antiseptics and disinfectants are used extensively in hospitals and other health care settings for a variety of topical and hard-surface applications. In particular, they are an essential part of infection control practices and aid in the prevention of nosocomial infections. Increasing concerns over the potential for microbial contamination and infection risks have led to increased use of antiseptics and disinfectants in health care premises, food processing facilities, public amenities and in many general consumer applications. A wide variety of active chemical agents (or "biocides") are used in the above-mentioned areas, many of which have been used for hundreds of years for antisepsis, disinfection, and preservation (for a review, see McDonnell and Russell 1999).

A. Ivask (✉)
National Institute of Chemical Physics and Biophysics, Laboratory of Molecular Genetics, Tallinn, Estonia

University of California Center for Environmental Implications of Nanotechnology, Los Angeles, CA, USA
e-mail: angela.ivask@kbfi.ee

S. George
University of California Center for Environmental Implications of Nanotechnology, Los Angeles, CA, USA

School of Chemical and Life Sciences, Nanyang Polytechnic, Singapore
e-mail: saji_GEORGE@nyp.gov.sg

O. Bondarenko • A. Kahru
National Institute of Chemical Physics and Biophysics, Laboratory of Molecular Genetics, Tallinn, Estonia
e-mail: olesja.bondarenko@kbfi.ee; anne.kahru@kbfi.ee

N. Cioffi and M. Rai (eds.), *Nano-Antimicrobials*,
DOI 10.1007/978-3-642-24428-5_9,

Based on the type of biocidal active ingredients, antimicrobial agents can be broadly divided into two types: organic and inorganic. One of the earliest used organic antiseptics was phenol (carbolic acid) that Joseph Lister started to use in operating theatres for sterilization of surgical instruments in 1865, which significantly reduced mortality rates associated with surgical procedures. Most of the currently used antibiotics are also of organic nature as they have originally been synthesized by various microorganisms (mostly fungi) to fight their competitors. The inorganic metal-based disinfectants/drugs, however, have an even longer history: silver has been used to fight infections as far back as the days of ancient Greece and Egyptian civilizations. In World War I, before the advent of antibiotics, silver compounds were used to prevent and treat infections. The journal *Lancet* (May 31, 1919) published information on the drugs used in Paris hospitals at that time "...Certain popular drugs have only recently been inscribed on the official list, e.g., novocain in 1908, *colloidal silver in 1909*, arsenobenzol in 1911, novarsenobenzol in 1912, and galyl in 1915. Other new remedies still on trial in Paris hospitals include certain *colloidal metals* and organo-therapeutic extracts prepared for intravenous medication...". Moreover, copper materials have been used since 2200 BC to produce drink and food storage vessels which due to their antimicrobial properties prevented spoilage (Dollwet and Sorenson 1985). The onset of zinc as antimicrobial is, however, more recent: since 1977, ZnO has been authorized by US FDA (http://www.fda.gov/) in externally applied drugs as well as in cosmetics. Currently, ZnO is used, e.g., as an antiseptic in surgical tapes, deodorants, and soaps, to provide topical relief in skin irritation, diaper rash, minor burns, and cuts. The increasing interest in the use of metals and metal oxides as antimicrobials is attributed to their ability to withstand harsh process conditions, durability and the sustained antimicrobial action which are often the shortcomings of organic antimicrobial compounds.

Along with the rapid development of nanotechnology witnessed during the past 10 years and due to a vast number of studies showing higher effectiveness of nano-sized materials than their micro- or macro-sized counterparts, the metal-containing nano-antimicrobials may present revolutionizing applications in consumer and patient care products. The higher activity of nano-sized materials compared to their 'larger' analogues has been mainly attributed to the ir relatively higher specific surface area and, thus, high amount of active molecules/atoms present on the surface. As an example, a 1-nm nanoparticle would have ~76% of its atoms present on the surface. Thus, the *physical dimensions* as well as the *chemical composition and stability* determine the reactivity of each nanomaterial and govern their specific type of nano–bio interaction. In the following paragraphs, we discuss the current knowledge about the contribution of physical dimensions and chemical characteristics (including dissolution) of the most widely applied and/or most promising metal-containing nano-antimicrobials, Ag, ZnO, TiO_2, and CuO, in their antimicrobial activity. We also present and discuss the (bio)analytical methods that have been developed and/or applied to discriminate between the antimicrobial effects mediated by metal dissolution and particles *per se*.

9.2 Antimicrobial Action of Metal-Containing Nano-Antimicrobials with Special Emphasis on Their Dissolution

As previously mentioned, metal-containing antimicrobials have been considered to bring a revolutionary breakthrough in hygiene as well as in medical applications. However, while we start to enjoy the primary benefit of nanotechnology-based improvements in antimicrobial applications, one of the main questions that need to be answered is: how likely are these nanomaterials to exert their toxic effects on non-target biological systems? This question can only be answered based on extensive knowledge about the detailed mechanisms of action of these metallic nano-antimicrobials. Therefore, it is of utmost importance to understand the key mechanisms of action of already applied or potential antimicrobial compounds *prior* to their large-scale application. Yet, the early studies on metal-containing nanomaterials toxicity did not address the issue but rather reported empirical observations on cellular viability. Only since 2007 have major efforts been made to link the toxicological and antimicrobial potency of nanomaterials to their physico-chemical properties. The observations have indicated that the potency of metal-containing nanomaterials is controlled by their physical dimensions and, most importantly, their chemical stability. Examples of the properties related to nanomaterials' (NMs') physical properties that have been demonstrated to modulate their toxicity are: *size* (Panáček et al. 2006) (Choi and Hu 2008) and *shape* (Pal et al. 2007). Examples of toxicologically important properties related to NMs' chemical composition and stability are: *surface coating* (El Badawy et al. 2010), *doping* (George et al. 2010) and *dissolution* (Cioffi et al. 2005; Morones et al. 2005; Franklin et al. 2007; Smetana et al. 2008; Heinlaan et al. 2008; Kahru et al. 2008; Rai et al. 2009; Jiang et al. 2009; Allaker 2010). Although all these NMs properties may be observed separately, the final toxicological outcome of a nanomaterial is usually due to the joint action (that may lead to synergy) between the key physico-chemical properties. *Metal ion dissolution* from metal-containing nanomaterials may be considered as one of the most important key factors in their toxicity. Due to the fact that bacteria have rigid cell envelopes and do not have internalization mechanisms for supramolecular and colloidal particles, the effect of nano-sized materials on bacterial cells is mostly restricted to the effects at or near the cell wall. Differently from bacteria that are unicellular prokaryotic organisms, most eukaryotic systems have highly developed molecular machineries for internalization of nano- and microscale particles. Therefore, in eukaryotic systems, the physical properties of the NMs may have a markedly greater role than in prokaryotes. Specific examples emphasizing the role of dissolution will follow below for each of the nano-antimicrobials separately, but at this stage, we wanted to emphasize that the dissolution rate of metal oxide NMs has been used in one of the very few nano-QSAR (quantitative structure–activity relationship) models currently available, as a single predictor for their toxicity to *E scherichia coli* in *in vitro* tests (Puzyn et al. 2011).

According to that model, the metal oxides (M) that had lower enthalpy (ΔH_{M+}) to form a gaseous cation (M^{n+}) in the reaction:

$$M(\text{solid}) = M^{n+}(\text{gas}) + n^{*}\,\bar{e}\Delta H_{M}{}^{+}, \tag{9.1}$$

are more likely to be transformed to cations and thus exert toxic effects to *E. coli*.

In the following sections, we give an overview about recent findings on mechanisms of toxic action of the most widely used and most promising metal and metal oxide nano-antimicrobials: TiO_2, Ag, ZnO and CuO.

9.2.1 Nano-TiO_2

9.2.1.1 Importance of Nano-TiO_2 as an Antimicrobial

Nano-TiO_2 is a semiconductor that shows antimicrobial properties during photoactivation and is probably the highest production volume nanomaterial (Mueller and Nowack 2008). The exact current production volumes for TiO_2 are relatively difficult to estimate, however, the current production volume of TiO_2 in USA is estimated to be between 7,800 and 38,000 t/year (Hendren et al. 2011). Robichaud et al. (2009) have estimated that the annual production of this nano metal oxide will reach 2.5 million tonnes by 2025.

The use of TiO_2 in different consumer products including food has a long history and as stated by Dr. Wetter in her presentation on behalf of ETC Group at US FDA Nanotechnology Public Meeting on October 10, 2006 (http://www.fda.gov/ScienceResearch/SpecialTopics/Nanotechnology/NanotechnologyTaskForce/ucm111425.htm): "…FDA approved TiO_2 as a food color additive as early as in 1966 with the stipulation that the additive was not to exceed 1% by weight and TiO_2 is also approved as a food packaging additive. Currently TiO_2 is being formulated at the nano-scale and the transparent particles are being used in clear plastic food wraps for UV protection. Apparently, this percent-by-weight limit set back in the 1960s for micro-scale TiO_2 particles is not relevant to today's nano-scale formulations since tiny amounts can produce large effects. And nano-scale TiO_2 in food is just one example…". In addition to the use of TiO_2 in coatings for its white color and UV protection of food, textiles or human skin, the TiO_2-coated surface also has a strong antimicrobial activity when exposed to sunlight. For the first set of applications, TiO_2 natural form, rutile, is used, whereas for antimicrobial applications, a rarer TiO_2 polymorph, anatase, is used (Mueller and Nowack 2008). A large number of studies on the photocatalytic disinfection efficiency of TiO_2 for water purification (Wei et al. 1994), as well as for self-cleaning surfaces (Gelover et al. 2006), has been published. For example, Chen et al. (2008) showed that when TiO_2 particles were attached onto bacterial surfaces, fast antimicrobial effects were observed after UV illumination. Such laboratory research findings are being translated into commercial products: TiO_2 is already used in home air purifiers, e.g. 3Q Multistage Air Purifier and

NanoBreeze Room Air Purifier, to remove volatile organic compounds and kill bacteria. TiO_2 as an antimicrobial is suitable for large-scale antimicrobial applications because it is stable, relatively non-toxic by incidental ingestion, and is low-cost.

9.2.1.2 Evidence for Nano-TiO_2 Antimicrobial Properties

As reported by Kahru and Dubourguier (2010), toxicity of TiO_2 was considerably lower in comparison to other current and potential nano-antimicrobials: ZnO, Ag and CuO. However, it must be noted that, due to the requirement for photoactivation, the available toxicity data for nano-TiO_2 are relatively inconsistent. The reason for this may be varying light exposure conditions and illumination duration, and the test media, as well as TiO_2 concentrations used. Interestingly, our recent data (A. Ivask, unpublished data) showed that the antibacterial effect of TiO_2 is not linearly related to the applied dose and that addition of highly concentrated (>100 μg/mL) nano-TiO_2 aqueous suspension to a photoactivation experiment decreased its antibacterial effects. This may be the reason why TiO_2 exerts its optimal photocatalytic antimicrobial activity when immobilized on to a surface (Ireland et al. 1993). Currently, the inhibitory potential of TiO_2 against *Escherichia coli, Bacillus subtilis* (Ireland et al. 1993; Adams et al. 2006), *Staphylococcus aureus* (Tsuang et al. 2008), MRSA (methicillin-resistant *Staphylococcus aureus*) (Sunada et al. 1998; Wei et al. 1994), *Entercococcus hirae, Pseudomonas aeruginosa, Bacteriodes fragilis* (Tsuang et al. 2008) and natural bacterial community (Gelover et al. 2006) has been reported. The reported concentrations of TiO_2 required to affect bacterial viability usually vary between 100 and 1,000 μg/mL, depending on the size of the particles and the intensity and wavelength of the light applied for photoactivation (Wei et al. 1994). Gelover et al. (2006) showed that 15-min exposure to 87 μg/mL of TiO_2 was enough to completely inactivate fecal coliforms. On the other hand, 10,000 μg/mL of TiO_2 was reported as an effective concentration to inactivate *S. aureus, E. hirae and P. aeruginosa*, *B. fragilis* and *E. coli* after 50-min exposure to UV light (Tsuang et al. 2008). As mentioned above, these differences in effective concentrations may be due to the differences in exposure conditions and properties of the nanomaterials.

9.2.1.3 Modes of Antimicrobial Action of Nano-TiO_2

Toxicity and antimicrobial properties of TiO_2 have almost exclusively been linked to its photoexcitation under UV light. Upon UV light exposure, electrons in the valence band get excited to a conduction band leaving behind a hole. The conduction band electron and valence band hole can react with molecular oxygen and water molecules, respectively, to generate superoxide and hydroxyl radical. Thus, the most commonly formed ROS include hydroxyl radicals, superoxide and peroxide production under UV irradiation (Kikuchi et al. 1997). For a more detailed

discussion on the mechanisms of antibacterial action of TiO_2 nanoparticles, the reader is directed to the excellent review by Foster et al. (2011). In addition to bacteria, TiO_2 nanoparticles in combination with UV light have been shown to inactivate microorganisms such as blue-green algae *Anabaena*, *Microcystis*, and *Melosira* (Kim and Lee 2005) and *Chroococcus* sp. (Hong et al. 2005) by potentially destroying the algal cell surface. In addition, a specific aggregation of algal cells with TiO_2 particles leading to poorer growth or decreased photosynthetic ability of the algae have been reported by several groups (Aruoja et al. 2009; Sadiq et al. 2011). Toxicity data of TiO_2 are also available for a number of other (eco)toxicological model organisms. However, these data are often variable, which may be the result of different exposure conditions used as well as of different physico-chemical properties of TiO_2 used in the experiments (Menard et al. 2011).

9.2.1.4 The Role of Dissolution in Antimicrobial Action of TiO_2

Currently, no reports showing the release of metal ions from TiO_2 nanomaterials and their significant effects in toxicity have been published and, thus, the antimicrobial effect of this material may be attributed solely to its photocatalytic and surface redox properties. However, as TiO_2 nanoparticles have also shown toxicity to *Bacillus subtilis* and *E. coli* in dark conditions (Adams et al. 2006), the mechanisms of action of bactericidal properties of nano-TiO_2 warrants further investigations.

9.2.2 Nano-ZnO

9.2.2.1 Importance of Nano-ZnO as an Antimicrobial

ZnO is probably the second highest volume of metal-containing nanomaterials produced after TiO_2. As mentioned above, ZnO is topically used to provide relief in skin irritation, diaper rash, minor burns and cuts but also in cosmetics such as deodorants and soaps. Since nano-sized ZnO is believed to exert a higher efficacy than the micro- or macro-sized ZnO, the applications of nano-ZnO include packaging materials in the food industry (Tayel et al. 2011), dental applications to prevent biofilm formation (Allaker 2010), antimicrobial wallpaper (Ghule et al. 2006) or in textiles (Rajendran et al. 2010). ZnO-impregnated textiles have been shown to retain their antimicrobial properties even after 50 washing cycles (Rajendran et al. 2010).

9.2.2.2 Evidence for Nano-ZnO Antimicrobial Properties

The antibacterial activity of nano-ZnO has been demonstrated towards both Gram-negative and Gram-positive bacteria although at relatively high concentrations. The reported effective concentrations of nano-ZnO fall usually between 80 and

10,000 μg/mL depending on the observed endpoint and test conditions. EC_{50} values for nano-ZnO have been reported between 1.8 and 1,000 μg/mL (Adams et al. 2006; Brayner et al. 2006; Heinlaan et al. 2008; Gajjar et al. 2009; Baek and An 2011) whereas complete growth inhibition has been observed at higher concentrations even reaching 10,000 μg/mL (Ren et al. 2009; Applerot et al. 2009; Liu et al. 2009). The efficacy of nano-ZnO has also been shown towards yeast *Saccharomyces cerevisiae* at 120–130 μg/mL (Kasemets et al. 2009).

9.2.2.3 Modes of Antimicrobial Action of Nano-ZnO

Based on the current literature, three mechanisms leading to nano ZnO toxicity and antimicrobial effects may be pointed out: (1) *dissolution*, (2) *size*, and (3) *induction of reactive oxygen species* (ROS) (Table 9.1). As mentioned above, these mechanisms can be related to each other and also combined.

Dissolution of ZnO to Zn ions has been considered as the mechanism for (nano-) ZnO toxicity in a vast number of papers and these are discussed below (Sect. 9.2.2.4). Here, we discuss the evidence for size-related and ROS-dependent toxicity mechanisms of nano-ZnO.

Nanosize has been considered as an important property leading to nano-ZnO toxicity by Jones et al. (2008) and Applerot et al. (2009). In the first study, it was demonstrated that 5-nm initial-sized particles were five-fold more toxic than 50–70-nm particles (Jones et al. 2008), and the second study showed that 6.8-nm ZnO particles exerted much higher antibacterial activity than 260 or 800-nm particles (Applerot et al. 2009). In addition to the increased surface area of the smaller particles, smaller sized nano-ZnO has even been suggested and/or proven to enter the cells of *E. coli* and *S. aureus* (Brayner et al. 2006; Liu et al. 2009; Applerot et al. 2009) (Fig. 9.1b,c). The internalization of ZnO nanoparticles by bacterial cells is surprising since the sizes of nanoparticles are approximately 50 times larger than the pore sizes of the membrane pumps and, according to the available information, bacteria have no internalization mechanisms for supramolecular and colloidal particles. The authors suggested that possibly, the *de novo* formation of respective membrane channels for small nanoparticles takes place in real time (Applerot et al. 2009). Indeed, bacteria have shown to internalize <5-nm CdSe and CdSe/ZnS quantum dots, probably by oxidative damage of the cell membrane potentialized by light (Kloepfer et al. 2005).

The evidence for induction of ROS as one of the toxicity mechanisms of nano-ZnO has been presented by Sawai (2003), Ghule et al. (2006), Zhang et al. (2007), Applerot et al. (2009), and Ivask et al. (2010). Sawai (2003) even suggested the photocatalytic generation of hydrogen peroxide to be one of the primary mechanisms of ZnO toxicity. Indeed, ZnO is a semiconductor that upon absorbtion of photons transports its electrons between the valence and conduction band. The photogenerated electrons and electron holes undergo reactions with dissolved molecular oxygen, surface hydroxyl groups or adsorbed water molecules to form

Table 9.1 Selected studies reporting on the contribution of dissolved metal ions in antimicrobial effects of metal containing nanomaterials

Nanomaterial		Test organism	Toxicity endpoint	Quantity dissolved (method used for metal ion separation)	Contribution of dissolved ions in toxicity	Additional reported toxicity mechanisms	Reference
Type	Description						
Ag	Commercial, nano-Ag, <100 nm	*E. coli* bioluminescent cells	Inhibition of bioluminescence	3.3% of Ag solubilized (bioavailable Ag ions analyzed by cellular Ag biosensors)	100% of toxicity including ROS was caused by solubilized Ag ions.	ROS due to solubilized ions	Ivask et al. (2010)
	Commercial, nano-Ag, <100 nm	ROS inducible *E. coli*	Induction of bioluminescence by ROS	3.3% of Ag solubilized (bioavailable Ag ions analyzed by cellular Ag biosensors)	Nano-Ag induced more ROS than could be expected from Ag ions	ROS due to nanoparticles per se at subtoxic concentrations	Ivask et al. (2010)
	Citrate-stabilized nano-Ag, 10 nm	*E. coli*	Bacterial growth (number of cells)	0.1% of the total silver in nano Ag (filtration, 3,000 kDa cutoff)	Nano-Ag was 10^3–10^4 times more toxic than Ag dissolution predicted	ROS due to nanoparticles, enhanced intracellularization of nano Ag compared to Ag^+, intracellular release of ions	Lok et al. (2007)
	16 nm nano-Ag particles in carbon matrix	*E. coli, P. aeruginosa*	Bacterial growth (number of cells)	<5 μM (stripping voltammetry)	Nano-Ag was more toxic than respective concentration of soluble Ag salt	Accumulation of nano Ag in cell membrane and intracellularly	Morones et al. (2005)
	In-house SMAD synthesized nano-Ag, 3–100 nm	*E. coli*	10-minute decrease in viable colonies	Qualitative estimation (addition of NaCl and observation of white precipitate formation and reduction in toxicity)	Formation of Ag^+ was the only cause for nano-Ag toxicity	None	Smetana et al. (2008)
	Nano-Ag-coated plastic catheters	*E. coli, E. faecalis, S. aureus, P. aeruginosa, C. albicans*	Biofilm formation	15% of Ag release in 10 days (radioactive ^{110m}Ag released)	Catheter surface decreased bacterial biofilm formation; however no quantitative correlations with Ag release was performed	None	Roe et al. (2008)

	Polymer-immobilized nano-AgBr	*E. coli, B. cereus*	MIC, biofilm formation	2.8–3.65 ppm/g AgBr dissolved (filtration, 200 nm filter)	Toxicity of AgBr composites was due to the release of Ag ions to test media for prolonged periods	None	Sambhy et al. (2006)
	In-house synthesized nano-Ag, 3 nm	*E. coli, S. aureus, B. subtilis*	Growth inhibition	0.3% in DI water, and 4% in nutrient media (filtration, 200 nm filter)	Toxicity of nano-Ag was higher than respective amount of soluble Ag salt	Mechanical membrane damage	Ruparelia et al. (2008)
	In-house synthesized nano-Ag	yeast, *E. coli, S. aureus*	Growth inhibition	No Ag ions quantified	Nano-Ag and Ag ions exhibited similar effect towards *E.coli* at similar concentration	ROS generation	Kim (2007)
ZnO	Commercial ZnO, 30 nm	*V. fischeri*	Inhibition of bioluminescence	100% between 0.1 and 1 mg/L of ZnO (bioavailable Zn ions analyzed by cellular Zn biosensors)	100% of toxicity was due to solubilized Zn ions	None	Heinlaan et al. (2008)
	Commercial ZnO, 30 nm	*E. coli* bioluminescent cells	Inhibition of bioluminescence	100% between 0.1 and 1 mg/L of ZnO (bioavailable Zn ions analyzed by cellular Zn biosensors)	100% of toxicity was due to solubilized Zn ions	H_2O_2 in addition to solubilized Zn ions	Ivask et al. (2010)
	Commercial ZnO, 30 nm	ROS inducible *E. coli*	Induction of bioluminescence by ROS	100% between 0.1 and 1 mg/L of ZnO (bioavailable Zn ions analyzed by cellular Zn biosensors)	100% of toxicity was due to solubilized Zn ions	H_2O_2 in addition to solubilized Zn ions	Ivask et al. (2010)
	Commercial ZnO, 30 nm	*S. cerevisiae*	Growth inhibition	100% between 0.1 and 1 mg/L of ZnO (bioavailable Zn ions analyzed by	100% of toxicity was due to solubilized Zn ions	None	Kasemets et al. (2009)

(continued)

Table 9.1 (continued)

Nanomaterial		Test organism	Toxicity endpoint	Quantity dissolved (method used for metal ion separation)	Contribution of dissolved ions in toxicity	Additional reported toxicity mechanisms	Reference
Type	Description						
				cellular Zn biosensors)			
	Commercial ZnO	*P. chlororaphis*	Growth inhibition	15–30% (at pH 7.12 and 6–5, respectively) (centrifugation at 15,000 g)	Some toxicity was due to solubilized ions	None	Dimkpa et al. (2011)
	Commercial ZnO, <100 nm	*E. coli*	Viability, growth	1.90%, depending on dissolution media (centrifugation at 10,000 g 30 min, filtration through 200 nm)	All toxicity of ZnO was due to solubilized Zn ions	None	Li et al. (2011)
	Commercial and in-house synthesized, 20–30 nm	*E. coli, P. putida, B. subtilis*	Viability	30% of total Zn in nanomaterial (filtration, 100-nm filter)	All toxicity due to Zn ions, no nano-specific effect detected	None	Li et al. (2010)
	In-house synthesized ZnO	*E. coli, S. aureus*	Viability	Not quantified; 1.6–5 mg/L of Zn was considered as maximum solubilization from ZnO	No toxicity due to Zn ions, mainly due to membrane damage, $OH^{\bullet}$ production	Formation of $OH^{\bullet}$ on the nanomaterials surface	Applerot et al. (2009)
CuO	Polymer nanocomposite loaded with nano-CuO	*S. cerevisiae*, mold, *E. coli S. aureus*, *L. monocytogenes*	Growth inhibition	Qualitative (electro-thermal atomic absorption spectroscopy ETAAS)	Toxicity increased with increasing CuO (and, thus, Cu ion) concentration in the polymer-matrix	None	Cioffi et al. (2005)
	In-house synthesized, CuO, 7–17 nm	*E. coli*, *B. subtilis*, *S. aureus*	Growth inhibition	17% in rich media, 0.5% in water (not specified)	n.d	None	Ruparelia et al. (2008)

In-house synthesized Cu-doped TiO_2, 20 nm	*M. smegmatis; S. oneidensis*	Growth inhibition	Qualitative (ultracentrifugation, filtration, EDTA chelation)	100% of Cu doped to TiO_2 was in soluble form toxicity increased with increasing Cu doping in TiO_2	None	Wu et al. (2009)
Commercial CuO, 30 nm	*V. fischeri*	Inhibition of bioluminescence	33% (between 1 and 20 mg/L) (bioavailable Cu ions analyzed by cellular Cu biosensors)	Contribution from solubilized ions relatively high (almost 100%)	None	Heinlaan et al. (2008)
Commercial CuO, 30 nm	*E. coli*	Inhibition of bioluminescence	33% (between 1 and 20 mg/L) (bioavailable Cu ions analyzed by cellular Cu biosensors)	100% of toxicity was due to solubilized Cu ions	None	Ivask et al. (2010)
Commercial CuO, 30 nm	O_2^- inducible *E. coli*	Induction of bioluminescence by $O_2^{\bullet-}$	33% (bioavailable Cu ions analyzed by cellular Cu biosensors)	100% of ROS generation was due to solubilized Cu ions	O_2^- radicals were only due to solubilized Cu ions	Ivask et al. (2010)
Commercial CuO, 30 nm	H_2O_2 and DNA damage inducible *E. coli*	Induction of bioluminescence by H_2O_2 and ssDNA	20% (bioavailable Cu ions analyzed by cellular Cu biosensors)	100% of ROS generation was due to solubilized Cu ions	H_2O_2 and DNA damage were only due to solubilized Cu ions	O. Bondarenko et al. (unpublished data, 2011)
Commercial CuO, 30 nm	*S. cerevisiae*	Growth inhibition	33% (bioavailable Cu ions analyzed by cellular Cu biosensors)	50% of toxicity was due to solubilized Cu ions	ROS	Kasemets et al. (2009)
Commercial CuO, 33 nm	*P. chlororaphis*	Growth inhibition	0.25–2% at pH 6 and 7 (centrifugation)	Partial toxicity due to Cu ions	None	Dimkpa et al. (2011)

ROS reactive oxygen species

hydroxyl ($OH^{\bullet}$) and superoxide ($O_2^{\bullet -}$) radicals, as suggested by (Niazi and Gu 2009):

$$\begin{aligned} &ZnO + hv \rightarrow h_{vb}^{+} + e_{cb}^{-} \\ &O_2 + e_{cb}^{-} \rightarrow O_2^{\bullet -} \\ &H_2O + h_{vb}^{+} \rightarrow OH^{\bullet} + H^{+}, \end{aligned} \tag{9.2}$$

where e_{cb}^{-} is a conducting band electron and h_{vb}^{+} is the valence-band hole. Neal (2008) has suggested that ZnO-induced ROS may lead to disruption of bacterial membranes and thereby induce their porosity, which could further result in uptake of ZnO nanoparticles *via* the damaged cell wall. Membrane deformations and impaired morphology of bacterial cells after exposure to nano-ZnO have been demonstrated by Zhang et al. (2007) and Li et al. (2011) (see also Fig. 9.1). Also, electrochemical

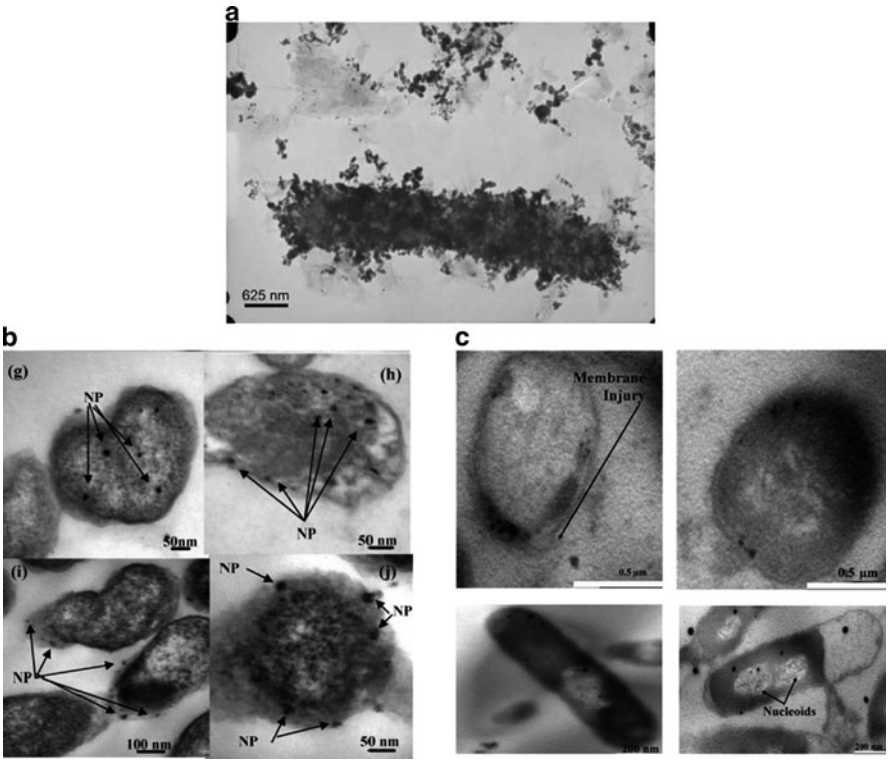

Fig. 9.1 *Evidence for surface attachment and internalization of nano-ZnO by bacterial cells.* (**a**) Attachment of ZnO nanoparticles to *E. coli* surface (cells were exposed to 100 μg/mL of ZnO) (Reprinted from Jiang et al. 2009. With permission from Elsevier). (**b**) Intracellular nano-ZnO in *E. coli* cells (ZnO particles are shown with *black arrows*) (Reprinted from Brayner et al. 2006. Copyright American Chemical Society). (**c**) Internalization of nano-ZnO (primary size 6.8 nm) in *S. aureus* (*upper row*) and *E. coli* (*lower row*) cells (Reprinted from Applerot et al. 2009. Copyright Wiley; reproduced with permission)

measurements using a model 1,2-dioleoyl-sn-glycero-3-phosphocholine (DOPC) lipid monolayer suggest a tight interaction between ZnO nanoparticles and the bacterial membranes and resulting membrane damage (Zhang et al. 2007).

9.2.2.4 The Role of Dissolution in Antimicrobial Action of Nano-ZnO

ZnO could certainly be suggested as a metal-containing nanomaterial the effect of which has most often been directly connected with its dissolution and shedding of the toxic heavy metal ion, Zn^{2+} (Table 9.1). Hereby, it is interesting to note that the Material Safety Data Sheets for ZnO and nano ZnO (CAS 1314-13-2) state that this material is *poorly soluble* or even *insoluble* or the solubility data are missing, leading, thus, to erroneous conclusions and precautions by end-users. Dissolution of ZnO has been believed to occur during surface hydrolysis of this metal oxide:

$$\mathrm{ZnO(solid)} + 2\mathrm{H}^{+} = \mathrm{Zn}^{2+} + \mathrm{H_2O} \tag{9.3}$$

The first paper discussing the dissolution of ZnO as a reason for toxicity was by Franklin et al. (2007) using freshwater algae. These authors demonstrated that, even at pH 7.6, a very rapid dissolution of ZnO bulk and nano forms took place, and at 100 μg of ZnO/mL, at least 15 μg/mL was present as Zn ions. They showed that, if dissolved Zn from ZnO was used as the concentration unit, the obtained EC_{50} values for nano-ZnO and a soluble Zn salt coincided. Li et al. (2011) showed almost complete dissolution of ZnO nanomaterials in most commonly used bacteriological media, LB (rich organic media) and Minimal Davis (mineral media with citrate) media – at 100 μg of nano-ZnO/mL, 90% and 40% of it was detected as soluble Zn, respectively. Interestingly, solubility of nano ZnO in other environments – saline, water and PBS (phosphate-buffered saline) – was markedly lower but still 12%, 7% and about 1% of nano ZnO was present as dissolved ions, respectively. Li et al. (2010) showed marked dissolution of Zn ions from nano-ZnO – at 1 μg/mL, the dissolution rate was 0.3 μg/mL being completely responsible for their observed antibacterial effects as proven by parallel testing with a soluble Zn salt. Thus, the authors concluded that no measurable 'nano effect' was associated with ZnO bacterial toxicity. Liberation of Zn ions from ZnO nanoparticles has been shown as the sole mechanism for their antibacterial (Adams et al. 2006; Heinlaan et al. 2008; Ivask et al. 2010; Wu et al. 2010), algaecidal (Aruoja et al. 2009) and antifungal activity (Kasemets et al. 2009). Similarly to antibacterial effects of ZnO, systematic investigations into the mammalian toxicity of ZnO nanoparticles also pointed towards the dissolution and release of Zn^{2+} ion as the principal mechanism of toxicity (Xia et al. 2008; George et al. 2010). Limiting the dissolution of ZnO in aqueous media by iron doping reduced the toxicity of ZnO in mammalian cells and higher organisms (Xia et al. 2008; George et al. 2011). In addition to ZnO dissolution due to physico-chemical processes in the surrounding environment, cellular activities (excretion of acids as metabolic by-products, for example) may also lead

to its dissolution. For example, Fasim et al. (2002) showed that the bacteria *P. aeruginosa* can solubilize nano-ZnO and other solid Zn salts, and total dissolution of 14 mM (1,140 μg/mL) ZnO in 3 days was achieved. It is interesting to note that along with ZnO dissolution, pH of bacterial culture decreased to 3.5 which by itself could be one additional reason for the observed ZnO dissolution. Finally, we want to emphasize that the solubility of nano-ZnO may not necessarily be solely due to its nano-property. This is supported by the fact that at least up to a certain concentration of ZnO, several studies have shown similar dissolution and also toxicological effects of bulk and nano-ZnO materials (Heinlaan et al. 2008; Kasemets et al. 2009; Aruoja et al. 2009; Ivask et al. 2010; Li et al. 2011). Keeping this finding in mind, the past consideration of "insolubility" of ZnO is even more surprising.

9.2.3 Nano-Ag

9.2.3.1 Importance of Nano-Ag as an Antimicrobial

Silver has probably the longest application history among all the metal-containing antimicrobials. Even today, its antimicrobial application is increasing due to its efficacy, high durability and resistance to high temperature processing. One can safely say that, among all antimicrobial nanomaterials, *nano-Ag* is used in the highest number and variety of consumer products from cosmetic applications, clothing, shoes, and detergents to dietary supplements, surface coatings, respirators, water filters, cell phones, laptop keyboards and children's toys (Maynard 2007). About 300 of over 1,000 nanomaterial-containing consumer products currently on the market contain nano-Ag (www.nanotechproject.org). Although the history of intended use of Ag in consumer products dates back to 2000, nano-Ag-containing products have been on the market for hundreds of years. Nanoscale silver colloids, known under different trade names such as Collargol, Argyrol, and Protargol entered the market in the early part of the twentieth century and over a 50-year period their use became widespread. These nanosilver products were sold as over-the-counter medications and also used by medical doctors to treat various diseases such as syphilis and other bacterial infections. Moreover, after the establishment of the EPA in 1970, all silver registrations in the next 23 years until 1993 were for nano-silver (colloidal silver) or for silver nanocomposites (for a review, see Nowack et al. 2011). Warningly, the increasing use of colloidal silver in over-the-counter drugs and also in these available the Internet have increased reports in cases of argyria in people, i.e. skin coloration due to hematogenous spread after topical application (Sebastian Tomi et al. 2004) or ingestion of *argentum proteinatum* (colloidal silver) preparations (White et al. 2003). Nowadays, nano-sized silver preparations may be used in a number of forms – as metallic silver nanoparticles, silver-impregnated zeolite powders and activated carbon materials, dendrimer–silver

complexes, silver–titanium dioxide composite nanopowders, and silver nanoparticles coated onto polymers like polyurethane (Marambio-Jones and Hoek 2010).

9.2.3.2 Evidence for Nano-Ag Antimicrobial Properties

There are numerous publications showing the toxicity of nano-Ag to microorganisms (Kahru and Savolainen 2010). The list of microbes that have been reported as sensitive to nano-Ag consist of but is not limited to bacteria *E. coli, Staphylococcus aureus, S epidermis, Leuconostoc mesenteroides, Bacillus subtilis, Klebsiella mobilis*, and *K. pneumoniae, Enterococcus faecalis,* and *Pseudomonas aeruginosa* (Balogh et al. 2001; Sondi and Salopek-Sondi 2004; Kim 2007; Kim et al. 2007; Benn and Westerhoff 2008; Chen and Chiang 2008; Falletta et al. 2008; Jung et al. 2008; Roe et al. 2008; Ruparelia et al. 2008; Smetana et al. 2008; Vertelov et al. 2008; Yoon et al. 2008; Zhang et al. 2008; Kim et al. 2009a; El-Rafie et al. 2010), yeasts *Candida albicans* and *Saccharomyces cerevisiae,* fungi *Aspergillus niger* and *Penicillium citrinum* (Kim et al. 2007; Roe et al. 2008; Vertelov et al. 2008; Zhang et al. 2008; Kim et al. 2009b). Given that nano-Ag is effective towards such a wide range of microbes, it is highly likely that nano-Ag would also adversely affect useful microflora, e.g., present in soil, human skin and gut. Although the variety of nano-Ag materials that have been tested for antimicrobial effects is high; ranging from uncoated to coating-stabilized and polymer-embedded nanoparticles, generally the toxicity of nano-Ag as measured by bacterial growth inhibition falls between 0.2 and 300 μg/mL. Gajjar et al. (2009) showed a decrease in CFU (colony-forming units) of *Pseudomonas putida* at 0.2 μg of nano-Ag/mL, while Vertelov et al. (2008) showed growth inhibition of *E. coli* and *S. aureus* cells by 5 μg of differentially coated Ag nanomaterials/mL. Kvitek et al. (2008) showed that the MIC (minimal inhibitory concentration) for non-coated nano-Ag aqueous suspension for *S. aureus, E. faecalis, E. coli*, and *P. aeruginosa* ranged from 1.6 to 13.5 μg/mL. Smetana et al. (2008) showed a decreasing effect of 30 μg/mL aqueous dispersion of Ag nanomaterials to *E. coli*, CFU after 10 min of exposure. Raffi et al. (2008) showed that *E. coli* cells were completely inhibited by 60 μg of nano-Ag/mL, Sambhy et al. (2006) demonstrated growth inhibition of *E. coli* and *Bacillus cereus* by 50 μg of AgBr-cationic polymer-embedded particles/mL and Ren et al. (2009) reported that 100 μg of nano-Ag/mL was MIC for *S. aureus*, *E. coli* and *P. aeruginosa*. The only study reporting very different antimicrobial activity of nano-Ag is by Kim et al. (2007) who showed that 13.4-nm silver nanoparticles prepared by reduction with borohydride had MIC of 0.00043 μg/mL for *E. coli*, 0.00356 μg/mL for *S. aureus* and 0.001 μg/mL for yeast isolated from bovine mastitis.

9.2.3.3 Modes of Antimicrobial Action of Nano-Ag

Despite the vast number of papers discussing the antimicrobial effects of nano-Ag, there is still no common agreement concerning the mechanisms of the observed

effects. Generally, there are three mechanisms that are brought up to explain the antibacterial mechanism of Ag nanomaterials: (1) *release of silver ions* by dissolution (Hwang et al. 2008; Smetana et al. 2008; Rai et al. 2009); (2) *generation of reactive oxygen species* (ROS) by reactions taking place on nano-Ag surface with molecular oxygen (Kim et al. 2007; Hwang et al. 2008) and (3) *surface reactivity* due to different crystal defects on nanomaterials surface (Morones et al. 2005; Pal et al. 2007) (Table 9.1). Whether all these mechanisms function independently or synergistically, is still unclear. Although there is evidence for the generation of ROS, and papers are emerging showing the importance of surface reactivity in nano-Ag toxicity, the final toxic outcome is most likely a joint/additive (or, potentially, even synergistic) effect of all these factors combined with the 'nano' effect of these particles and dissolution. For example, even when Navarro et al. (2008) observed that the toxicity of Ag nanoparticles for *Chlamydomonas reinhardtii* was higher than what could be predicted based on their dissolution rate, they finally suggested that the enhanced toxicity of nano-Ag was due to increased dissolution of Ag^+ ions when Ag nanoparticles interacted with H_2O_2 generated by the algae. Another study by Lok et al. (2007) showed that Ag nanoparticles exerted 1,000-fold higher antimicrobial activity than could be predicted from their dissolution rate (0.1% of nanoparticles were in dissolved form). Again, the authors suggested that the final cause of the observed toxicity were still dissolved Ag ions released upon internalization of 10 nm nano-Ag. Additional evidence for nano-Ag 'nano effect' combined with dissolution was presented by Choi and Hu (2008). These authors observed an increased bactericidal activity of 5-nm-sized Ag nanoparticles compared to what could be expected based on their dissolution and suggested that, upon direct contact with membranes, local dissolution of nano-Ag occurred and the released Ag ions acted on membrane-bound enzymes of nitrifying bacteria. Indeed, as also discussed by Morones et al. (2005) and Sondi and Salopek-Sondi (2004), direct association of nano-Ag with bacterial membranes and subsequent local release of Ag ions may be involved in nano-Ag toxicity (Fig. 9.2). Also, Kim et al. (2007) and El Badawy et al. (2010) have shown that efficient binding of Ag nanomaterials onto bacterial surfaces is a prerequisite for their toxicity. El Badawy et al. (2010) even presented a clear decrease in nano-Ag toxicity to *E. coli* when the surface charge was converted to negative by certain surface coatings and, thus, the binding efficacy of nanoparticles onto membranes was decreased. Ruparelia et al. (2008) suggested that the bound Ag nanomaterials may exert toxic effects due to membrane damage. Liau et al. (1997) evidenced that this large-scale membrane damage by degrading the cell surfaces and forming pits as shown by Sondi and Salopek-Sondi (2004) (Fig. 9.2c) could be due to ROS production by Ag nanomaterials. Production of ROS by Ag nanomaterials either related to the dissolution or surface reaction with molecular oxygen has been evidenced in a number of papers (Kim 2007; Lok et al. 2007; Ivask et al. 2010). ROS induction by nano-Ag is indeed a property that has also been observed using other types of organisms, e.g., in fish cell lines (Carlson et al. 2008; Farkas et al. 2010).

The importance of surface reactivity in nano-Ag toxicity is a relatively less studied phenomenon. Morones et al. (2005) noticed that, among Ag nanoparticles with different crystal lattices, the crystal facet with a {111} lattice indices was

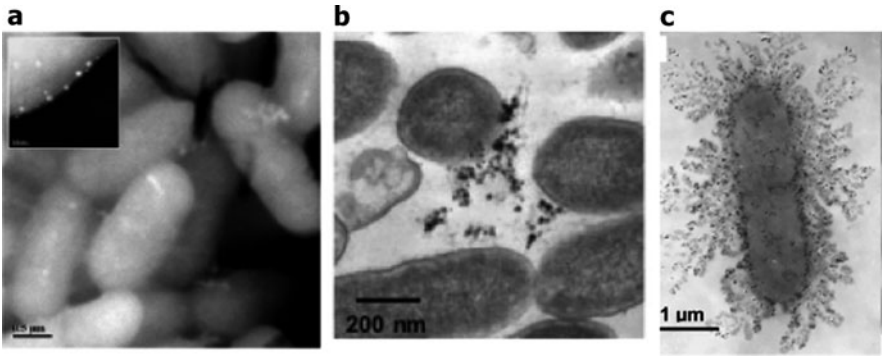

Fig. 9.2 *Association of nano Ag with bacterial cells.* (**a**, **b**) Transmission electron micrographs (TEM) of *Pseudomonas aeruginosa* cells after treatment with 100 μg/mL of nano Ag. Attachment of nano-Ag on bacterial surface (**a**, **b**) and the resulting membrane disruption (**b**) may be seen (Reprinted from Morones et al. 2005. Copyright IOP Science). (**c**) TEM images of *Escherichia coli* cells treated with 50 μg/mL of nano Ag. Degraded outer membrane structures (lipopolysaccharides) may be observed (Reprinted from Sondi and Salopek-Sondi 2004. With permission from Elsevier)

preferred for interactions with the bacterial cell membrane and, in particular, sulfur-containing membrane proteins. They inferred that the {111} crystal facet, which has high-atom-density compared to other lattice structures, leads to direct interaction with the bacterial membrane. Later, studies by Pal et al. (2007) demonstrated that crystal structure indeed has an influence to the toxicity of Ag nanoparticles to bacterial cells wherein the rod-shaped and triangular particles were markedly more toxic for bacteria than the spherical structures. According to their explanation, the planar nano-Ag structures were more reactive due to the high proportion of crystallographic faces available for nanoparticle–bacteria contact. Indeed, among different shapes, particles with a higher proportion of exposed crystallographic faces showed higher electrocatalytic reactivity (Bansal et al. 2010), which could be due to increased frequency of crystal defects in these structures. Although these surface reactivities are not yet discussed in relevance to the toxicity of Ag nanoparticles with different crystal structures, data emerging from our laboratory suggest the role of crystal defects in enhanceing the toxicity of plate-shaped Ag nanoparticles.

9.2.3.4 The Role of Dissolution in Antimicrobial Action of Nano-Ag

Regardless of the myriad of different opinions, there is no doubt that the release of Ag ions either alone or in combination with other, previously discussed mechanisms is one of the most important factors determining the toxicity of nano-Ag. Differently from nano-ZnO, the chemical reactions behind the dissolution of Ag involve redox reactions either in the presence of oxygen (Fan and Bard 2001; Le Pape et al. 2004; Smetana et al. 2008; Choi et al. 2008):

$$4Ag + O_2 + 2H_2O = 4Ag^+ + 4OH \tag{9.4}$$

or as suggested by AshaRani et al. (2008) in the presence of hydrogen peroxide originating from mitochondria of eukaryotic cells:

$$2Ag + H_2O_2 + 2H^+ = 2Ag^+ + 2H_2O \tag{9.5}$$

Marambio-Jones and Hoek (2010) hypothesized that a similar process involving hydrogen peroxide could also occur in bacterial membranes. As the dissolution of Ag either following reaction in Eqs. 9.4 or 9.5 involves transfer of electrons, formation of ROS, such as superoxide anions ($O_2^{\bullet -}$) and hydroxyl radicals ($OH^{\bullet}$), in this process is very likely. On the other hand, Park et al. (2009) also showed that dissolved Ag^+ ions could induce $O_2^{\bullet -}$ in bacterial cells. Therefore, the induction of intracellular ROS by nano-Ag observed in studies by Kim et al. (2007), Lok et al. (2007) and Ivask et al. (2010) may be due to the combination of these factors.

The summary of selected studies on nano-Ag dissolution and its impacts on its toxicity is given in Table 9.1. For example, in the case of nano-Ag incorporating surface coatings, release of ions has been directly related to their antimicrobial activity, and in order to prolong and control that release of antimicrobial Ag ions, embedding of Ag nanomaterials, e.g., to cationic polymer poly(4-vinyl-*N*-hexylpyridinium bromide), has been used (Sambhy et al. 2006). Shedding of Ag from Ag nanoparticles is also evidenced by the fact that some ligand-capped silver nanoparticles – although highly stable and monodisperse in suspension – were less bioactive, and authors concluded that the capping agent hindered the release of silver ions (Smetana et al. 2008). By using bacterial Ag sensor cells, Ivask et al. (2010) showed that all the observed antimicrobial effects of nano-Ag were due to solubilized ions. Lok et al. (2006) showed that the proteomic response of *E. coli* to nano-Ag and $AgNO_3$ was similar. Both compounds showed altered expression profile of envelope and stress response proteins. This kind of change in protein expression level could be expected as Ag ions are known to interact with membrane-bound thiol-rich respiratory chain enzymes (Dibrov et al. 2002) leading to collapse in the transmembrane pH gradient and membrane electric potential (Holt and Bard 2005). Finally, we want to emphasize that the dissolution of Ag ions from nano-Ag may take place either in the surrounding environment following the chemical equilibria or at the particle–cell membrane interface. The latter is especially likely because of the oxidizing environment on bacterial surface as discussed with Eq. 9.5. As these processes – abiotic dissolution of nano Ag and its dissolution after binding to bacterial surfaces or even internalization – may occur simultaneously, the separation of Ag dissolution from other factors important in nano Ag toxicity is a complicated task.

9.2.4 Nano-CuO

9.2.4.1 Importance of Nano-CuO as an Antimicrobial

Although not yet widely applied in commercial products, Cu nanomaterials are discussed in this chapter due to their high antimicrobial potential. Cu has long been known for its antimicrobial effects and was applied, e.g., in antifungal treatments and antifouling agents. Cu nanomaterials have been proposed as antimicrobials in polymer nanocomposites (Cioffi et al. 2005) that could serve as antimicrobial surfaces for packaging and in medicine. Borkow et al. (2010) used *nano-CuO* in wound dressings and showed its antimicrobial and antifungal properties by removing 99.9% of microbial cells even at high microbial loads within minutes. Akhavan and Ghaderi (2010) immobilized Cu and CuO nanoparticles in silica thin films to produce antimicrobial surfaces.

9.2.4.2 Evidence for Nano-CuO Antimicrobial Properties

Compared with the previously discussed nano-antimicrobials, CuO has the least number of toxicity data available (Kahru and Savolainen 2010). However, its effectiveness towards *Staphylococcus aureus, Escherichia coli, Pseudomonas aeruginosa, P. putida, Bacillus subtilis,* and *Vibrio fischeri* has been demonstrated (Heinlaan et al. 2008; Gajjar et al. 2009; Ren et al. 2009; Baek and An 2011). The effective concentrations for this nanomaterial towards microbes reported in different publications vary from 10 to 5,000 μg/mL, whereas in most of the studies, toxicity has been observed between 10 and 100 μg/mL. Gajjar et al. (2009) showed that 10 μg of CuO/mL decreased both the CFU (colony forming unit) and bioluminescence of a recombinant *P. putida* strain. A similar concentration has been shown to inhibit bioluminescence in recombinant *E. coli* strain by Ivask et al. (2010), and Heinlaan et al. (2008) showing that 80 μg/mL decreased the natural bioluminescence of *V. fischeri* by 50% and at 200 μg/mL, 100% inhibition was observed. Kasemets et al. (2009) showed that 30 μg/mL of nano-CuO inhibited the growth of yeast *Saccharomyces cerevisiae*. And 28–65 μg/mL has been shown as EC_{50} of nano-CuO for *E. coli, B. subtilis*, and *S. aureus* (Baek and An 2011). Relatively lower toxicity of nano-CuO for *S. aureus, E. coli,* and *P. aeruginosa* ranging from 100 to 5,000 μg/mL was reported by Ren et al. (2009), which, however, may be due to their experimental setup that involved the observation of inhibition by nanomaterials only after the transfer of bacteria to fresh growth media.

9.2.4.3 Modes of Antimicrobial Action of Nano-CuO

Based on the currently published articles, it is still disputable whether the observed antimicrobial effects of CuO nanomaterials are due to specific 'nano effects' or due to the release of Cu ions and their mediated toxicity (Table 9.1). Very few reports

are available on the mechanism of bactericidal action of copper nanoparticles. However, based on the current literature, three mechanisms for antimicrobial action of nano CuO can be proposed: (1) *metal dissolution*, (2) specific *nano-effects* and (3) induction of *reactive oxygen species* (ROS) (Table 9.1). The effect of dissolution in toxicity of nano-CuO is discussed in the next section (Sect. 9.2.4.4.). The 'nano effect' as a reason for nano-CuO toxicity was exclusively highlighted by Baek and An who reported that the dissolution rate of nano-CuO did not explain its toxicity (Baek and An 2011). However, the mechanisms behind this observed 'nano effect' were not proposed. A 'nano-effect' combined with solubility as a toxicity mechanism has been presented by Heinlaan et al. (2008) and Ivask et al. (2010). Using *E. coli* and *V. fischeri*, these authors demonstrated that the nano-size of CuO resulted in higher solubility and' thus, toxicity (see Sect. 9.2.4.4). Induction of intracellular ROS by CuO particles in *E. coli* bacteria has been observed by Ivask et al. (2010) and by O. Bondarenko (unpublished data, 2011; see Table 9.1). However, these authors also proved that the ability of CuO nanoparticles to induce ROS is again clearly dependent on the dissolution rate of nano CuO; similar results but for abiotic systems have been shown by Rice et al. (2009).

9.2.4.4 The Role of Dissolution in Antimicrobial Action of Nano-CuO

As already mentioned, the importance of dissolution of Cu nanomaterials in determining their antibacterial properties has been highlighted in many papers (Trapalis et al. 2003; Ruparelia et al. 2008; Ren et al. 2009; Akhavan and Ghaderi 2010) (see summary in Table 9.1) and indirect evidence on this process has been reported. Cioffi et al. (2005) showed that increasing the load of nano-Cu in polymer nanocomposites increased the bactericidal activity of the material towards *Saccharomyces cerevisiae*, *Escherichia coli*, *Staphylococcus aureus*, *Listeria monocytogenes* and molds. With increasing nano-Cu load in polyvinylmethyl ketone, there was a concomitant increase in the solubilized Cu, which apparently is thought to be the reason for toxicity of these materials. Similarly, decreased release of Cu ions from polyvinylidenefluoride–nano-Cu composite showed reduced antimicrobial activity. Thus, the authors concluded that, by using differently controlled Cu release in different nano-CuO–polymer composites, it is possible to control their antimicrobial properties. The studies on Cu-doped Ti and Se nanoparticles showed that the antibacterial action of the particles correlated well with the content of Cu ions in the coating (Trapalis et al. 2003). The addition of 20 mg/L ethylenediaminetetraacetic acid (EDTA) abolished the toxicity of Cu-TiO_2, showing that their toxicity to bacteria *Mycobacterium smegmatis* and *Shewanella oneidensis* was fully caused by Cu ions (Wu et al. 2009). Indirect evidence on participation of dissolved Cu ions in CuO toxicity has also been shown with eukaryotic cells. Studer et al. (2010) showed that if the carbon layer preventing the dissolution of Cu ions was used to coat nano-CuO, it was significantly less toxic.

Only a few studies have been aimed to differentiate the effects of dissolved Cu ions and the CuO particles *per se* in detail. Heinlaan et al. (2008) quantified the

dissolution of Cu ions from nano-CuO and reported that the toxicity of nano-CuO to *V. fischeri* was entirely explained by the dissolved Cu ions. In a similar experimental setup, Ivask et al. (2010) showed that the toxicity of nano-CuO to *E. coli* cells was due to solubilized ions. As discussed in Sect. 9.2.3.4, induction of ROS has been shown as one of the mechanisms of toxicity of nano-CuO. Mostly, this property of nano-CuO may be attributed to dissolved Cu ions that are well known for their redox reactive properties (Kimura and Nishioka 1997). The fact that intracellular ROS induced by nano-CuO were solely the result of solubilized Cu ions was shown by Ivask et al. (2010) and O. Bondarenko et al. (unpublished data, 2011; see Table 9.1) by the parallel use of biosensor systems that allowed the detection of dissolved ions and ROS in parallel. The formation of both, superoxide anions and hydrogen peroxide by nano-CuO was detected. These studies were supported by Rice et al. (2009) who showed by using cell-free media that the generation of $OH^{\bullet}$ radicals was solely due to Cu ions solubilized from nano-CuO.

9.3 Environmental Parameters Affecting the Dissolution of Metal-Containing Nano-Antimicrobials

Although in previous chapters we discussed mainly the inherent properties of nanoparticles that determine their dissolution, the final dissolution of each of the nanomaterials depends on the conditions used in the test. Perhaps one of the best examples on how the test conditions may affect the dissolution of metal-containing nanoparticles has been given by Li et al. (2011) who studied the dissolution of ZnO nanomaterials in different test media and observed almost complete dissolution (90% at 100 μg of nano-ZnO/mL) in LB medium (bacterial medium containing organics) and very high dissolution rate (40% at 100 μg of nano-ZnO/mL) in Minimal Davis media (bacterial mineral medium containing citrate). For comparison, dissolution of nano-ZnO in saline, water or PBS (phosphate-buffered saline) was 12%, 7% and about 1%, respectively. The authors suggested that the affinity of Zn to the ligands present in these media was responsible for nanomaterial dissolution. The authors suggested that organic ligands in LB media and citrate in Minimal Davis media were the reasons for high solubility of nano ZnO and the low solubility of ZnO in PBS was due to the formation and immediate precipitation of Zn-phosphate complexes. As these complexes were removed when nanoparticles and dissolved ions were separated (using centrifugation combined with filtration, see Sect. 9.4), the final dissolved amount of Zn in PBS was very low. Proteins and organic substances have also been shown to increase the dissolution of nanoparticles of ZnO, CdSe, iron oxides, aluminium oxides and oxyhydroxides as well as CuO nanoparticles in earlier studies (Xia et al. 2008; Käkinen et al. 2011), and also explained by the organic ligand-enhanced dissolution.

Ag ion dissolution is determined by several factors such as nanomaterial surface functional groups (Liu et al. 2010), level of dissolved oxygen, temperature and

presence of organics (Liu and Hurt 2010). Differently from Zn^{2+} ion, which is relatively soluble, Ag^{+} easily forms complexes with most of the inorganic anions. The pK values of Ag complexes with different inorganic ligands are 9.75 for chloride, 4.9 for sulfate, 49 for sulfide, and 7.8 for hydroxide (Choi et al. 2008; Gao et al. 2009). Thus, as suggested by Jin et al. (2010), even if Ag ions are solubilized from nano-Ag material, there is a high possibility that these ions re-precipitate forming insoluble complexes with inorganic ligands. Therefore, nanomaterials in aqueous suspensions must be considered as a dynamic system where the apparent speciation is controlled by the aquatic media pH, redox potential, and ionic composition as well as exposure to light.

As a final note, we would like to emphasize that in case of nanomaterials the dissolution is also dependent on the agglomeration/aggregation state of the material. Thus, in addition to controlling the dissolution as such, an environmental factor also determines the dispersion state of the nanomaterial. For example, high salt concentration that is known to decrease the electrical double layer (Nel et al. 2009) and thus, cause nanomaterial aggregation, is perhaps acting also as a limitation for dissolution process due to loss of surface area. pH of the medium close to the nanomaterials isoelectric point also promotes nanoparticle aggregation but its effect on dissolution depends on the speciation properties of the respective metal.

9.4 Currently Used Methods to Separate Dissolved Metal Ions from Metal Containing Nano-Antimicrobials

As discussed above, there is much evidence available that suggests the importance of dissolved metal ions in the toxicity of metal-containing nano-antimicrobials. However, often the presented evidence does not allow the clear differentiation between the roles of dissolved ions and 'nano-specific' effects in the observed toxic properties. Thus, the experimental design is of utmost importance in mechanistic studies of nano-antimicrobials and nanomaterials in general. The suggested design would include the combination of measurement of dissolved metals by analytical methods, including parallel experiments with a soluble metal salt, and experiments with re-engineered materials to deliberately decrease or increase the solubility of the nanomaterial. Measurement of dissolved metal ions is, however, a key step in this experimental setup that requires a *prior* separation of nano-sized non-dissolved materials and solubilized metal ions. It should be emphasized that this task is not the most straightforward as the extremely small size of nanomaterials may cause difficulty in separating particles from solubilized metal ions and their potential complexes with organics present in the test media. Luckily, in most aqueous test environments that contain salts (e.g., microbial media), nanomaterials agglomerate heavily enabling their easier separation. However, the presence of individual nano-sized particles in these agglomerated samples cannot be ruled out and care should be taken when using any separation techniques.

Selection of a method to be used for nanomaterial–dissolved ion separation depends on the nature of the material. Usually, in cases of polymer/surface immobilized nanomaterials, no special separation techniques have been used and the presence of metals in overlaying water or media as analyzed by analytical techniques has been used to judge the level of metal dissolution. In a study by Roe et al. (2008), radioactive isotope ^{110m}Ag was used instead of common analytical detection techniques to measure the fraction of solubilized metals from a nano-Ag-containing polymer. Metal solubilization has also been analyzed based on their characteristics to form certain complexes. For example, due to its nature to form (visually opaque) chloride complexes, NaCl at 0.5 g/mL has been used to detect solubilized Ag ions from Ag nanomaterials (Smetana et al. 2008). A similar principle was applied by Rice et al. (2009) who used spectrophotometric measurement of Cu chelated by oxalic acid bis(cyclohexylidene hydrazide) to quantify solubilized Cu ions.

In this section, we introduce in detail some of the most commonly applied and perhaps most appropriate techniques for separation of dissolved metal ions from metal nanoparticles: *centrifugation* and *filtration*. We also discuss *metal ion chelation* as a method to determine whether the observed toxicity of nanomaterials was due to metal dissolution. In addition, we discuss some methods that may be used for speciation analysis of the dissolved metals: *assessment of labile and bioavailable metal ions* and *models that may be used for metal speciation analysis*.

9.4.1 Separation of Dissolved Metal Ions by Centrifugation

Centrifugal force leads to the sedimentation of particles while leaving the dissolved ions in the solution which can then be detected using analytical techniques. When selecting an appropriate condition for centrifugation, both the size and density of the nanomaterials has to be taken into account. Kaegi et al. (2008) showed that centrifugation at 330 g for 6 minutes is enough to sediment particles with size up to 1.8 μm if their density is 1.1 g/cm^3, particles with size up to 410 nm if their density is 2.7 g/cm^3 and particles with size up to 300 nm if their density is 4.2 g/cm^3. Two hours of centrifugation at 2,700 *g* was enough to sediment particles of less than 130 nm with a density of 1.1 g/cm^3, particles of less than 30 nm with a density of 2.7 g/cm^3 and particles of less than 20 nm with a density of 4.2 g/cm^3 (Kaegi et al. 2008). Thus, by simple centrifugation at low to moderate speeds, it is possible to separate particles as small as 20 nm from the nanomaterial suspension. A relatively low centrifugal speed was also used by Fasim et al. (2002) who isolated Zn dissolved from ZnO nanomaterials by 20-min centrifugation at 2,000 g. However, many studies have applied relatively high centrifugal speeds to ensure the sedimentation and separation of nanomaterials. Dimkpa et al. (2011) used a higher speed and longer duration of centrifugation (15,500 g for 30 min) for ion separation from commercial CuO and ZnO nanomaterial suspensions. However, they calculated that the actual time needed to sediment the nanoparticles at that speed was 5 min.

Midander et al. (2009) and Wu et al. (2010) used centrifugation at 19,000 g in combination with filtration (200 nm) to ensure the separation of Cu ions from CuO nano-suspensions. Indeed, as centrifugation could be considered as procedurally difficult and a technique with relatively low resolution power for size separation, the combination of this technique with other separation methods could be suggested.

9.4.2 Separation of Dissolved Metal Ions by Filtration

Filtration of nanomaterial suspension through membranes with controlled pore size is another method to separate metal-containing nanomaterials and solubilized ions. By selecting a filter with an appropriate pore size, it is possible to control the size of particles that pass the membrane or will be retained. There is a selection of filters available ranging from micro-sized pores from 0.1 to 1 μm to ultrafiltration (pore size around 0.01 μm) and nanofiltration (pore size around 0.001 μm). In addition to pore size, the material used to fabricate the filter is of importance as contamination or sorptive loss of the metals can become important at low (nanomolar) concentrations (Handy et al. 2008).

Filtration procedures have been discussed in detail by Behnke (1983) and Buffle et al. (1992). In most of the published reports on nanomaterial separation, filtration through 0.2-μm (i.e. 200-nm) filters has been used. There are reports showing the use of a 200-nm filter to separate nano CuO and Cu ions (Ruparelia et al. 2008; Wu et al. 2009). Baek and An (2011) used 200-nm nylon material filter to separate solubilized ions from ZnO, CuO, NiO and Sb_2O_3 nanomaterials in LB media without *prior* centrifugation. Li et al. (2011) used combined centrifugation (30 min at 10,000 g) and filtration through a 200-nm filter to separate solubilized Zn ions from ZnO nanomaterials. Heinlaan et al. (2011) used filtration of CuO suspensions through 100-nm polyethersulfone (PES) filters to separate solubilized Cu ions from nanomaterials. Interestingly, these authors showed that when filtration is applied as a single method to separate dissolved metal ions and nanomaterials, a 100-nm pore size may not be small enough cutoff to eliminate the presence of all nanomaterials. Indeed, they showed that, in the filtrates, a fraction of nanoparticles below 100 nm was present. A 100-nm pore-size filter was also used to separate dissolved Zn from ZnO nanomaterials by Li et al. (2010). These authors showed that application of a 100-nm pore size produced a similar yield to centrifugation at 15,000 g or dialysis through a 3,000-Da membrane. A similar comparison was done by Franklin et al. (2007) who showed that dialysis through a 1,000-Da cutoff filter that should restrict the passage of nanomaterials well below nanometer size yielded similar results to filtration of a nano-ZnO suspension through a 100-nm pore size filter. Differential results showing either complete or incomplete separation of nanomaterials from dissolved ions by using micro-sized filtration may be due to the differential dispersion state of nanomaterials. If the particles aggregate to $>$100 nm before filtration, the filter will certainly set a suitable limit to entrap the

particles; however, in the case of smaller particles, the cutoff may not be small enough.

Compared to macro-sized filtration, dialysis may provide a more complete separation method for small nanoparticles. For example, the molecular weight cutoff of 7,500 Da in dialysis membranes corresponds to 1-nm particles, 75,000 Da to 10-nm particles and 750,000 Da to 100-nm particles. Although dialysis offers an accurate degree of separation for particles and solutes, this procedure often involves scaling up of the test procedure and the dilution of the sample. This may change the dissolution kinetics of the nanomaterial, and therefore the results may deviate from the actual situation in the toxicity test. Thus, perhaps a more accurate method for metal ion separation is centrifugal ultrafiltration where the sample is centrifuged through a dialysis membrane. For example, Navarro et al. (2008) used centrifugation of silver nanomaterials suspensions at 3,000 g for 30 min through a 3,000-Da membrane and considered the filtered concentration of Ag as thesoluble fraction. Also, 3,000-Da centricon membranes were used to separate dissolved Ag ions by Lok et al. (2007).

9.4.3 *Qualitative Determination of the Presence of Dissolved Metal Ions by Chelation*

Chelation, i.e. complexation of free metal ions in suspensions of metal-containing nanomaterials has also been used as a method to separate the effects of nanomaterials and their dissolved metal ions. However, this method only offers a qualitative proof for the presence of dissolved ions, as the addition of a chelating agent either removes or does not remove the observed toxic effect of the nanomaterial. Usually, a chelating compound is added to the nanomaterial suspension and its biological effects are evaluated in comparison with nanosuspensions with no chelator added. If addition of a chelating compound removes or decreases the observed adverse effects, the toxicity of the metal-containing nanomaterial may at least be partially attributed to its solubility.

The most popular chelating compounds for metallic compounds are sulfur-containing molecules that have been shown to efficiently bind metal ions. For example, SH-groups in cysteine (Fig. 9.3) have been used to chelate Ag ions from Ag nanomaterials. Indeed, the addition of cysteine abolished the toxic effects

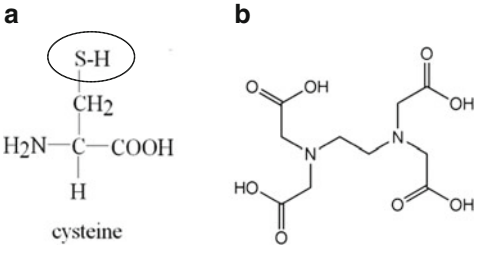

Fig. 9.3 *Structure of cysteine* (**a**) *and EDTA* (**b**) *molecules*. Sulfide group of cysteine reacting with metal ions is indicated, in the case of EDTA metal ions form coordinative bonds with nitrogen and oxygen cluster

of Ag nanomaterials to a green algae (Navarro et al. 2008). In another study, the effect of inorganic ligands on Ag ion complexation was studied, and it was shown that of the tested ligands, SO_4^{2-}, S^{2-}, Ci^{-}, PO_4^{3-} and EDTA (ethylenediaminetetraacetic acid), only S^{2-} showed efficacy in decreasing nanosilver toxicity. By adding a small aliquot of sulfide that was stochiometrically complexed with nano-Ag, the nanosilver toxicity to nitrifying organisms was reduced by up to 80% (Choi et al. 2009).

While in the case of Ag ions, sulfide anions were the most effective complexing agents and EDTA did not prove particularly efficient, Cu ions, including those liberated from CuO nanomaterials, were effectively chelated by EDTA (Wu et al. 2009). Actually, every metal may have its specific chelator ('specific antidote'): for Cu, a specific chelator is bathocuproine (1,10-dimethyl-4,7-diphenyl 1,10-phenanthroline disulfonate) which has been used to specifically complex Cu ions from nano-CuO (Dimkpa et al. 2011).

9.4.4 *Speciation of Dissolved Metals by Detection of Free and Labile Metal Ions*

In addition to the determination of total dissolved fraction of metals from metal-containing nanomaterials, the speciation of dissolved metal ions may be of interest. This is important because not all (even soluble) metal complexes formed in aqueous systems are equally toxic. The most reactive and toxic form of the metal is its free ion. However, when some organic components or even inorganic phosphates are present in the media, the amount of free ions usually markedly decreases and most of the dissolved metal in the sample may exist in the form of different organic or phosphate complexes. Knowledge about free and complexed metal species has been considered very valuable in environmental risk assessment (International Council on Mining and Metals 2007). However, as the nano-research is just in its infancy, and there are serious issues connected with attempts to separate the total solubilized fraction of metals, the sophisticated models and measurements necessary for gaining information about metal speciation have not yet been fully applied in the nano-field.

The techniques to separate free and labile metal ions were established for metal speciation in environmental samples such as soils and sediments decades ago (Pesavento et al. 2009). Due to the fact that environmental samples usually contain a range of colloidal or nanosized particles, these samples may be relatively similar to nanomaterial suspensions (Ivask et al. 2010) and thus, the techniques for free and labile metal ion detection may also be applicable in case of metal-containing nanomaterials.

Broadly, the techniques used to separate the free and labile metal ions may be categorized into electrochemical methods such as voltammetric techniques detecting the current from free/labile metals on the surface of an electrode, and non-electrochemical methods based on ion exchange, complexing resins or micro-

extraction. The working principles of some of these methods, stripping voltammetry, diffusive gradients in thin films (DGT) and ion selective electrode (ISE), are shown in Fig. 9.4. As stated earlier, the application of these techniques has not yet been established for nanomaterial suspensions, which may be due to the relatively sophisticated experimental design or low sensitivity of some of the methods. For example,

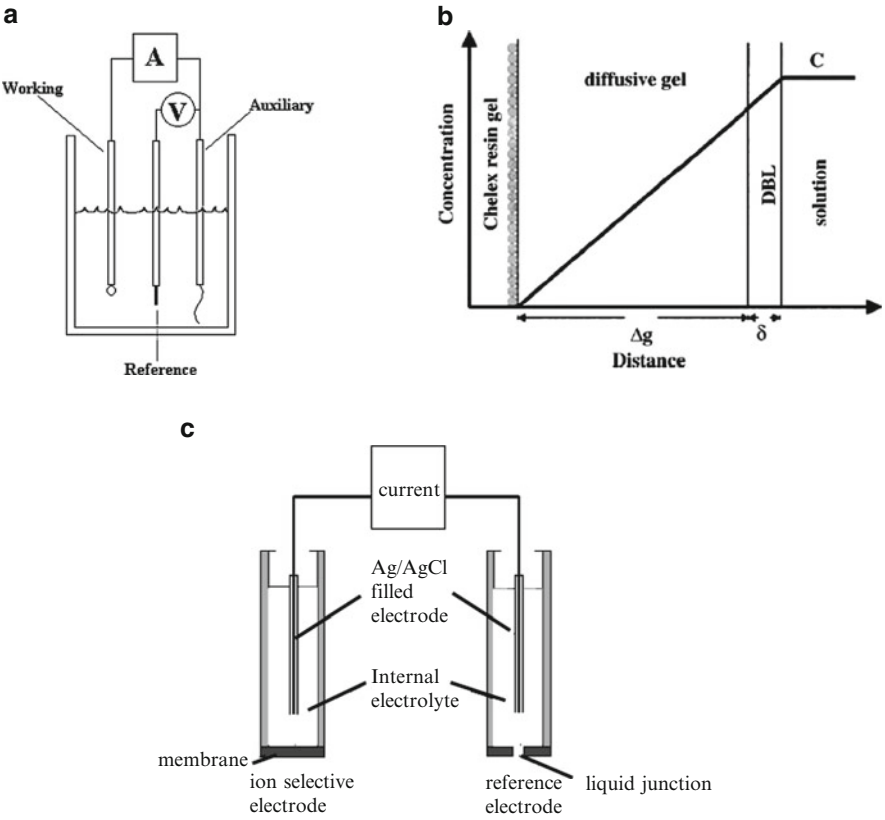

Fig. 9.4 *Metal speciation techniques commonly used for metal speciation in environmental studies*. (**a**) Stripping voltammetry is based on binding of the free/labile metals on the working electrode (usually a mercury film/drop) during a deposition step and a following oxidation of the deposited metals during a stripping step. The potential at which the stripping occurs indicates the nature and concentration of the analyte. (**b**) DGT technique based on passive sampling of free/labile metal species by a device incorporating hydrogel and a metal-binding resin, e.g., Chelex. As the resin is selective for free or weakly complexed metal species, analysis of passed metal concentrations provides a proxy for the labile fraction of metals in solution (Reprinted from Pesavento et al. 2009. With permission from Elsevier). (**c**) Ion-selective electrode is based on the measurement of the potential generated across a metal-specific membrane. The difference in potential of ion selective electrode and reference electrode upon immersing into a sample indicates the passage of charged metal ions through the membrane. Differently from stripping voltammetry and DGT that detect free and labile metal forms, ISEs are capable of detecting only free metal ions

the detection limits for ISEs fall usually between 10^{-6}–10^{-8} M that may not be enough for low-concentration samples (Pesavento et al. 2009).

There are a few papers reporting on the application of voltammetric methods or micro-extraction methods such as stripping voltammetry, DGT and ISE in the separation of solubilized metal ions from metal-containing nanomaterials. Navarro et al. (2008) used both, ISE and DGT to separate Ag ions from Ag nanoparticles. These authors showed that the results from these two different techniques were comparable and agreed with the results obtained by membrane dialysis of the samples, all indicating that 1% of Ag dissolved from 0.006 μg/mL Ag nanomaterial was in soluble form. Choi et al. (2008) used Ag ISE to separate dissolved and immobilized nano Ag when they synthesized Ag nanomaterials and colloids by $AgNO_3$ reduction. Stripping voltammetry was used for the specific quantification of Ag ions released from Ag nanomaterials by Morones et al. (2005). These authors found a relatively low concentration of silver solubilized from nano-Ag suspension with the maximum being less than 0.5 μg/mL. Käkinen et al. (2011) used Cu-ISE and bacterial Cu-biosensor in parallel, to study the speciation of Cu in suspensions of CuO nanoparticles. They showed that the speciation of nano-CuO in toxicological test systems was not only determined by the complexation of Cu ions but also by differential dissolution of nano-CuO in different test conditions leading to a new speciation equilibrium.

In addition to separation of free and labile metal ions by electrochemical techniques and semipermeable membranes or hydrogels, there are specific chemicals available that bind certain free ions. For example, quantification of Cu ions released from CuO was quantified by Cu ion binding to bathocuproine disulfate (Dimkpa et al. 2011). This chemical, a derivative of 1,10-phenantroline, may be successfully used to bind and colorimetrically detect Cu(I) between 0.1 and 10 μg/mL as it forms a red complex at physiological pH.

9.4.5 Models Used for Speciation of Dissolved Metals

As mentioned above, speciation of metals is an important factor in their apparent toxicity, but the respective models/calculations are not often used in nano-safety research. In previous paragraphs, we discussed some of the practical approaches that could be used to study the speciation of dissolved metal-containing nanomaterials. Here, we discuss some of the most promising speciation models. As in the case of speciation techniques, the speciation models have been primarily developed for environmental risk assessment (International Council on Mining and Metals 2007). These models are based on the equilibrium between the stability of free metal ions and of complexes that may be formed between the metal ion and the potential ligands in the study environment. The most widely used speciation models in environmental studies are WHAM (Windermere Humic Aqueous Model) (http://windermere.ceh.ac.uk/Aquatic_Processes/wham/) that allow the modeling of the aqueous interactions between metal ions and humic substances, and Visual Minteq (http://www2.lwr.kth.se/English/OurSoftware/vminteq/) that allows the modeling

of the aqueous interactions between metal ions and selected inorganic and organic ligands. No widely used speciation model is currently available for soils; for sediments, the SEM-AVS (Simultaneously Extracted Metal–Acid Volatile Sulfides) concept (Allen et al. 1991) has been used. Perhaps the most straightforward of these models is Visual Minteq. Indeed, a recent paper by Li et al. (2011) has applied this model to calculate the speciation of Zn that was dissolved from ZnO nanoparticles. In this case, the authors determined the total dissolved amount of Zn and then determined the speciation of this dissolved fraction in their test media. The amount of main anions and cations as well as organic ligands (such as citrate) were fed into the Visual Minteq model. Unfortunately, the results were not compared with toxicological tests or alternative speciation tests.

9.4.6 Speciation of Dissolved Metals by Detection of Bioavailable Metals Using Cellular Biosensors

As discussed above, formation of different metal complexes between the dissolved metal ions released from metal-containing nanomaterials and test media components may result in a decrease in toxicity due to the formation of non-bioavailable complexes. To predict the bioavailable fraction of metals, models like FIAM (Free Ion Activity Model) (Campbell 1995) and BLM (Biotic Ligand Model) (Paquin et al. 2002) have been applied in environmental risk assessment studies. These models take into account the chemical speciation as well as the affinity of certain biological ligands (e.g., on the biological surface, such as fish gills) that may facilitate the entrance of metal ions into the cells, to calculate the bioavailable, i.e., potentially toxic, fraction of metals. These models are, however, relatively sophisticated and have not so far been applied for nanomaterials.

There are very few tools available that allow the direct measurement of bioavailable metals. Here, we describe a novel approach involving recombinant metal-specific microbial sensors that has been used by Heinlaan et al. (2008), Kasemets et al. (2009), Aruoja et al. (2009) and Ivask et al. (2010) to quantify the bioavailable fraction of metals from metal-containing nanomaterials (including Ag, ZnO and CuO discussed in this chapter). This approach can be used as an analytical tool, and pre-separation of the particles from the solubilized fraction is not obligatory. As this methodology is relatively new, the methodological nuances of the approach will be discussed here. The analytical basis of this method is cellular biosensors that are recombinant microbes responding specifically towards certain heavy metals by increased bioluminescence. The bioluminescent response is induced, however, only if the particular heavy metal crosses the cell biological envelopes and enters the cytoplasmic space, that is if the metal is accessible or bioavailable to the sensing system. Mostly, the sensors are based on bacteria (Ivask et al. 2009) but also on yeast cells (Leskinen et al. 2003). These recombinant constructs contain genetic elements in which a metal-binding transcriptional regulator and its regulated promoter originating from microbial precisely regulated resistance

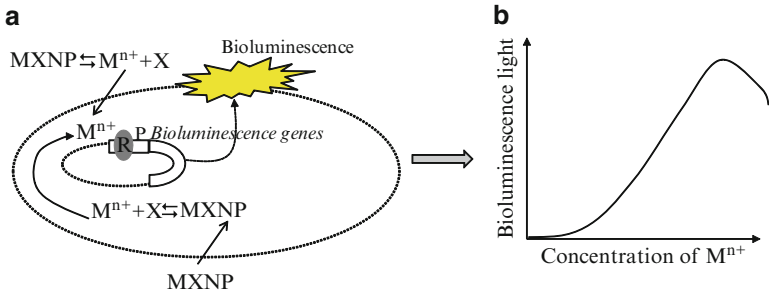

Fig. 9.5 *Working mechanism of a cellular metal ion biosensor.* (**a**) Metal ions (M^{n+}), released from metal-containing nanomaterials extracellularly or by intracellular dissolution bind a protein functioning as a transcriptional regulator (*R*). Regulator R binds a promoter (*P*), which is fused with bioluminescence encoding genes allowing the expression of the latter. The transcriptional regulator binds only certain metal ions and, thus, results in metal-specific expression of bioluminescence-encoding genes and resulting bioluminescence production. (**b**) With increasing metal ion concentration, the bioluminescence increases until the metal-binding transcriptional regulator is saturated (stable high bioluminescence is achieved) and/or a toxic concentration for the cell (bioluminescence decreasing) is reached. As only intracellular metal ions result in increased bioluminescence, this system may be detecting only bioavailable metals

systems towards heavy metals, are fused to bioluminescence-encoding (*lucFF* or *luxCDABE)* genes (Fig. 9.5).

Recombinant microbial heavy metal sensors have been developed for Cd, Pb, Hg, Cr, Ni, Co, Zn, Cu and As (for review, see Daunert et al. 2000) and have been widely used for heavy metal speciation studies in environmental analysis (Ivask et al. 2004, 2007, 2010; Kahru et al. 2005) offering a unique possibility for the quantification of bioavailable concentrations of target metals in complex environmental samples. The analysis scheme that can be used to evaluate the impact of solubilization of metals from metal-containing nanoparticles by recombinant metal-specific microbial sensors was first shown by Heinlaan et al. (2008). Since then, the methodology has been successfully used to demonstrate the toxic effect of solubilized Zn (using Zn-sensing bacteria) and Cu (using Cu-sensing bacteria and yeast) from nanoparticles of ZnO and CuO, respectively, towards algae (Aruoja et al. 2009), crustaceans and bacteria (Heinlaan et al. 2008; Ivask et al. 2010), protozoa (Mortimer et al. 2010) and yeast (Kasemets et al. 2009). Heinlaan et al. (2011) and O. Bondarenko et al. (unpublished data, 2011) have shown that solubilized Cu determined from nano-.CuO suspensions by these cellular Cu biosensors and filtration combined with analytical detection methods (AAS) were in good agreement ($R^2 = 0.88$). However, as a rule, the AAS values on dissolution of nano-CuO exceeded the values obtained by Cu-sensor bacteria. The difference could be explained by the fact that, after filtering the nanosuspensions through 100-nm pore-size filters the filtrate contained (<100 nm) CuO nanoparticles that did not induce the bioluminescence of Cu-sensor bacteria but were quantified during AAS analysis. Thus, these results indicate that, due to the complexity of separation of nanoparticles from the dissolved copper, the biosensors

seem to be even more relevant tools for the analysis of Cu ions than chemical methods to distinguish dissolved metal ions and insoluble (nano)materials.

9.5 Final Comments

In this chapter, we have discussed the potential mechanisms of toxicity of metal-containing nanomaterials keeping the main emphasis on their dissolution. Although dissolution of metal ions may be among the most important factors determining the toxicity of discussed nano-antimicrobials Ag, ZnO and Cu/CuO, their actual toxic outcome is certainly influenced by other physical/chemical properties of the nanomaterial: size, shape, surface characteristics and reactivity, photochemistry, etc. Figure 9.6 represents the summary of all potential factors leading to the toxic and antimicrobial effects of metallic nanomaterials that could be derived from the current literature. Due to the complexity of the process and inter-dependence of different physical and chemical properties in orchestrating the resultant reactivity and potency of nanomaterials, it is a daunting task to identify the contribution from

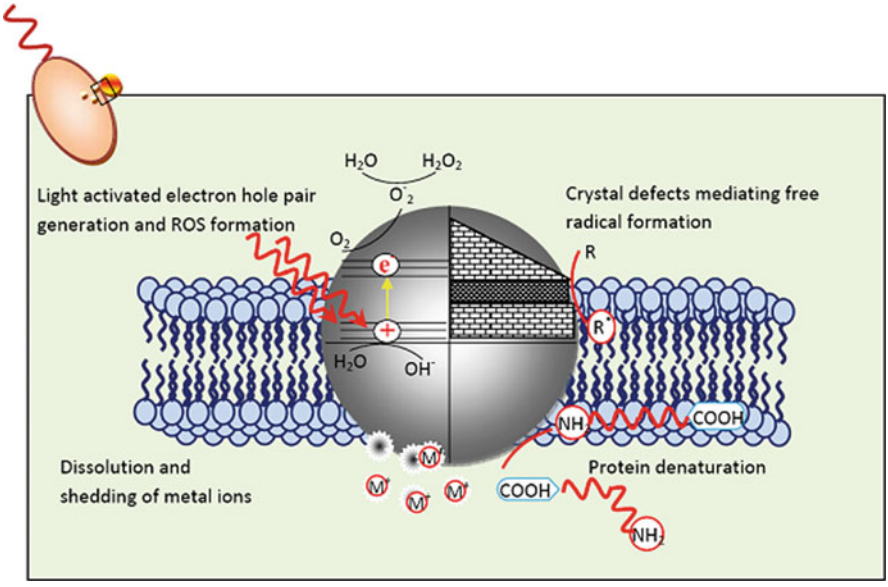

Fig. 9.6 *Properties of metal/metal oxide nanomaterials responsible for their toxic and antibacterial activities. Lower left corner*: dissolution of metal ions (M^+) from metal-containing nanomaterials. This process can take pace either extra- or intracellularly. *Upper right corner*: 'nano-specific' properties such as crystal defects, surface reactivity that lead to reactive free radical formation resulting in lipid peroxidation and protein deformation. *Upper left corner*: activation of nanomaterials by external agents such as UV illumination resulting in reactive oxygen species formation and their following reactions with biological molecules

each individual factor separately. Unveiling the functional relationship between physical/chemical properties of nanomaterials and toxicity may require the use of specifically designed nanomaterial libraries. Often this level of sophistication demands inter-disciplinary expertise wherein the key steps for establishing functional relationship between material property and toxicity are (1) synthesis and characterization of a library of nanomaterials with systematic variation in a critical nanoscale parameter, (2) identification of an appropriate toxicity endpoint in the target biological system, and (3) correlation of the toxicity data to the systematically varied physical/chemical parameter. We believe that only intelligent experimental planning including parallel testing of soluble metal forms and nanomaterials, measurement of dissolved metals by analytical methods, decreasing of dissolution rates e.g., by doping, would lead to meaningful information about dissolution as a separate factor in metallic nanomaterials toxicity. Unfortunately, even if all these possible controls are taken into account, some effects may remain unexplained. This may be due to e.g., locally increased dissolution and aggregation/disaggregation of nanomaterials, taking place in cellular-processes that are difficult if not impossible to measure by conventional experimental methods. Bearing this in mind, all the studies discussed in this chapter have a certain degree of simplification, but each of them provides a piece of information useful in assembling an integral picture about the behavior of metal-containing nanomaterials in biological systems.

Acknowledgements European Social Fund and Estonian Science Foundation programs Mobilitas, Do-Ra3, EU FP7 Project NanoValid (grant agreement No 263147) and projects ETF6975 and ETF8561 as well as Estonian Ministry of Science and Education project SF0690063s08 are acknowledged for the support.

References

Adams LK, Lyon DY, Alvarez PJJ (2006) Comparative eco-toxicity of nanoscale TiO_2, SiO_2, and ZnO water suspensions. Water Res 40(19): 3527–3532.

Akhavan O, Ghaderi E (2010) Cu and CuO nanoparticles immobilized by silica thin films as antibacterial materials and photocatalysts. Surf Coat Technol 205(1): 219–223.

Allaker RP (2010) The use of nanoparticles to control oral biofilm formation. J Dent Res 89(11): 1175–1186.

Allen HE, Fu G, Boothman W, DiToro D, Mahony JD (1991) Draft Analytical Method for Determination of Acid Volatile Sulfide in Sediment. U.S. Environmental Protection Agency, Washington, DC.

Applerot G, Lipovsky A, Dror R, Perkas N, Nitzan Y, Lubart R, Gedanken A (2009) Enhanced antibacterial activity of nanocrystalline ZnO due to increased ROS-mediated cell injury. Adv Funct Mater 19(6): 842–852.

Aruoja V, Dubourguier HC, Kasemets K, Kahru A (2009) Toxicity of nanoparticles of CuO, ZnO and TiO_2 to microalgae *Pseudokirchneriella subcapitata*. Sci Total Environ 407(4): 1461–1468.

AshaRani PV, Low Kah Mun G, Hande MP, Valiyaveettil S (2008) Cytotoxicity and genotoxicity of silver nanoparticles in human cells. ACS Nano 3(2): 279–290.

Baek YW, An YJ (2011) Microbial toxicity of metal oxide nanoparticles (CuO, NiO, ZnO, and Sb_2O_3) to *Escherichia coli, Bacillus subtilis* and *Streptococcus aureus*. Sci Total Environ 409(8): 1603–1608.

Balogh L, Swanson DR, Tomalia DA, Hagnauer GL, McManus AT (2001) Dendrimer – silver complexes and nanocomposites as antimicrobial agents. Nano Lett 1(1): 18–21.

Bansal V, Li V, O'Mullane AP, Bhargava SK (2010) Shape dependent electrocatalytic behaviour of silver nanoparticles. Cryst Eng Comm 12(12): 4280–4286.

Behnke U (1983) T. D. Brock: Membrane Filtration. A User's Guide and Reference Manual. 381 Seiten, 115 Abb., 27 Tab. Springer-Verlag, Berlin/Heidelberg/New York/Tokyo 1983, Preis: 87,- DM. Food/Nahrung 27(10): 1025.

Benn TM, Westerhoff P (2008) Nanoparticle silver released into water from commercially available sock fabrics. Environ Sci Technol 42(11): 4133–4139.

Borkow G, Okon-Levy N, Gabbay J (2010) Copper oxide impregnated wound dressing: biocidal and safety studies. Wounds 22(12): 301–310.

Brayner R, Ferrari-Iliou R, Brivois N, Djediat S, Benedetti MF, Fiévet F (2006) Toxicological impact studies based on *Escherichia coli* bacteria in ultrafine ZnO nanoparticles colloidal medium. Nano Lett 6(4): 866–870.

Buffle A, Perret D, Newman M (1992) The use of filtration and ultrafiltration for size fractionation of aquatic particles, colloids and macromolecules. In: Buffle A, Leeuwen HP (eds) Environmental Particles, vol. 1. Lewis Publishers, Boca Raton.

Campbell PGC (1995) Interactions between trace metals and aquatic organisms: a critique of the free-ion activity model. In: Tessier A, Turner DR (eds) Metal Speciation and Bioavailability in Aquatic Systems. Wiley, Chichester.

Carlson C, Hussain SM, Schrand AM, Braydich-Stolle K, Hess L, Jones KL and Schlager JJ (2008) Unique cellular interaction of silver nanoparticles: size-dependent generation of reactive oxygen species. J Phys Chem B 112(43): 13608–13619.

Chen CY, Chiang CL (2008) Preparation of cotton fibers with antibacterial silver nanoparticles. Mater Lett 62(21–22): 3607–3609.

Chen WJ, Pei-Jane T, Chen YC (2008) Functional Fe_3O_4/TiO_2 core/shell magnetic nanoparticles as photokilling agents for pathogenic bacteria. Small 4: 485–491.

Choi O, Hu Z (2008) Size dependent and reactive oxygen species related nanosilver toxicity to nitrifying bacteria. Environ Sci Technol 42(12): 4583–4588.

Choi O, Deng KK, Kim NJ, Ross JL, Surampalli RY, Hu Z (2008) The inhibitory effects of silver nanoparticles, silver ions, and silver chloride colloids on microbial growth. Water Res 42(12): 3066–3074.

Choi O, Clevenger TE, Deng B, Surampalli RY, Ross JL, Hu Z (2009) Role of sulfide and ligand strength in controlling nanosilver toxicity. Water Res 43(7): 1879–1886.

Cioffi N, Torsi L, Ditaranto N, Tantillo G, Ghibelli L, Sabbatini L, Bleve-Zacheo T, D'Alessio M, Zambonin PG, Traversa E (2005) Copper nanoparticle/polymer composites with antifungal and bacteriostatic properties. Chem Mater 17: 5255–5762.

Daunert S, Barrett G, Feliciano J, Shetty R, Shrestha S, Smith-Spencer W (2000) Genetically engineered whole-cell sensing systems: coupling biological recognition with reporter genes. Chem Rev 100(7): 2705–2738.

Dibrov P, Dzioba J, Gosnik KK, Häse CC (2002) Chemiosmotic mechanism of antimicrobial activity of Ag^+ in *Vibrio cholerae*. Antimicrob Agents Chemother 46(8): 2668–2670.

Dimkpa CO, Calder A, Britt DW, McLean JE, Anderson AJ (2011) Responses of a soil bacterium, *Pseudomonas chlororaphis* O6 to commercial metal oxide nanoparticles compared with their metal ions. Environ Pollut 159(7): 1749–1756.

Dollwet HHA, Sorenson JRJ (1985) Historic uses of copper compounds in medicine. J Trace Elem Med Biol 2(2): 80–87.

El Badawy AM, Silva RG, Morris B, Scheckel KG, Suidan MT,Tolaymat TM (2010) Surface charge-dependent toxicity of silver nanoparticles. Environ Sci Technol 45(1): 283–287.

El-Rafie MH, Mohamed AA, Shaheen TI, Hebeish A (2010) Antimicrobial effect of silver nanoparticles produced by fungal process on cotton fabrics. Carbohydr Polym 80(3): 779–782.

Falletta E, Bonini M, Fratini E, Lo Nostro A, Pesavento G, Becheri A, Lo Nostro P, Canton P, Baglioni P (2008) Clusters of poly(acrylates) and silver nanoparticles: structure and applications for antimicrobial fabrics. J Phys Chem C 112(31): 11758–11766.

Fan FRF, Bard AJ (2001) Chemical, electrochemical, gravimetric and microscopic studies on antimicrobial silverfilms. J Phys Chem B 106(2): 279–287.

Farkas J, Christian P, Gallego-Urrea JA, Roos N, Hassellov M, Tollefsen KE, Thomas KV (2010) Uptake and effects of manufactured silver nanoparticles in rainbow trout (*Oncorhynchus mykiss*) gill cells. Aquat Toxicol 101(1): 117–125.

Fasim F, Ahmed N, Parsons R, Gadd GM (2002) Solubilization of zinc salts by a bacterium isolated from the air environment of a tannery. FEMS Microbiol Lett 213(1): 1–6.

Foster H, Ditta I, Varghese S, Steele A (2011) Photocatalytic disinfection using titanium dioxide: spectrum and mechanism of antimicrobial activity. Appl Microbiol Biotechnol 90(6): 1847–1868.

Franklin NM, Rogers NJ, Apte SC, Batley GE, Gadd GE, Casey PS (2007) Comparative toxicity of nanoparticulate ZnO, bulk ZnO and $ZnCl_2$ to a freshwater microalga (*Pseudokirchneriella subcapitata*): the importance of particle solubility. Environ Sci Technol 41(24): 8484–8490.

Gajjar P, Pettee B, Britt DB, Huang W, Johnson WP, Anderson AJ (2009) Antimicrobial activities of commercial nanoparticles against an environmental soil microbe, *Pseudomonas putida* KT2440. J Biol Eng 3(9): 1–13.

Gao J, Youn S, Hovsepyan A, Llaneza VL, Wang Y, Bitton G, Bonzongo JCJ (2009) Dispersion and toxicity of selected manufactured nanomaterials in natural river water samples: effects of water chemical composition. Environ Sci Technol 43(9): 3322–3328.

Gelover S, Gómez LA, Reyes K, Teresa Leal M (2006) A practical demonstration of water disinfection using TiO_2 films and sunlight. Water Res 40(17): 3274–3280.

George S, Pokhrel S, Xia T, Gilbert B, Ji Z, Schowalter M, Rosenauer A, Damoiseaux R, Bradley KA, Mädler L, Nel AE (2010) Use of a rapid cytotoxicity screening approach to engineer a safer zinc oxide nanoparticle through iron doping. ACS Nano 4(1): 15–29.

George S, Xia T, Rallo R, Zhao Y, Ji Z, Lin S, Wang X, Zhang H, France B, Schoenfeld D, Damoiseaux R, Liu R, Lin S, Bradley KA, Cohen Y, Nel AE (2011) Use of a high-throughput screening approach coupled with in vivo zebrafish embryo screening to develop hazard ranking for engineered nanomaterials. ACS Nano 5(3): 1805–1817.

Ghule K, Ghule AV, Chen BJ, Ling YC (2006) Preparation and characterization of ZnO nanoparticles coated paper and its antibacterial activity study. Green Chemistry 8(12): 1034–1041.

Handy R, von der Kammer F, Lead J, Hassellöv M, Owen R, Crane M (2008) The ecotoxicol and chemistry of manufactured nanoparticles. Ecotoxicol 17(4): 287–314.

Heinlaan M, Ivask A, Blinova, Dubourguier HC, Kahru A (2008) Toxicity of nanosized and bulk ZnO, CuO and TiO_2 to bacteria *Vibrio fischeri* and crustaceans *Daphnia magna* and *Thamnocephalus platyurus*. Chemosphere 71(7): 1308–1316.

Heinlaan M, Kahru A, Kasemets K, Arbeille B, Prensier G, Dubourguier HC (2011) Changes in the *Daphnia magna* midgut upon ingestion of copper oxide nanoparticles: a transmission electron microscopy study. Water Res 45(179–190).

Hendren CO, Mesnard X, Dröge J, Wiesner MR (2011) Estimating production data for five engineered nanomaterials as a basis for exposure assessment. Environ Sci Technol 45(7): 2562–2569.

Holt K, Bard AJ (2005) Interaction of silver(I) ions with the respiratory chain of *Escherichia coli*: An electrochemical and scanning electrochemical microscopy study of the antimicrobial mechanism of micromolar Ag^+. Biochem 44(39): 13214–13223.

Hong J, Ma H, Otaki M (2005) Controlling algal growth in photo-dependent decolorant sludge by photocatalysis. J Biosci Bioeng 99(6): 592–597.

Hwang ET, Lee JH, Chae YJ, Kim YS, Kim BC, Sang BI, Gu MB (2008) Analysis of the toxic mode of action of silver nanoparticles using stress-specific bioluminescent bacteria. Small 4(6): 746–750.

Ireland JC, Klostermann P, Rice EW, Clark RM (1993) Inactivation of *Escherichia coli* by titanium dioxide photocatalytic oxidation. Appl Environ Microbiol 59(5): 1668–1670.

Ivask A, Francois M, Kahru A, Dubourguier H-C, Virta M, Douay F (2004) Recombinant luminescent bacterial sensors for the measurement of bioavailability of cadmium and lead in soils polluted by metal smelters. Chemosphere 22: 147–156.

Ivask A, Green T, Polyak B, Mor A, Kahru A, Virta M, Marks R. (2007). Fibre-optic bacterial biosensors and their application for the analysis of bioavailable Hg and As in soils and sediments from Aznalcollar mining area in Spain. Biosens Bioelectron 22: 1396–1402.

Ivask A, Rolova T, Kahru A (2009) A suite of recombinant luminescent bacterial strains for the quantification of bioavailable heavy metals and toxicity testing. BMC Biotechnol 9(1): 41.

Ivask A, Bondarenko O, Jepihhina N, Kahru A (2010) Profiling of the reactive oxygen species-related ecotoxicity of CuO, ZnO, TiO_2, silver and fullerene nanoparticles using a set of recombinant luminescent *Escherichia coli* strains: differentiating the impact of particles and solubilised metals. Anal Bioanal Chem 398(2): 701–716.

Ivask A, Dubourguier H-C, Põllumaa L, Kahru A (2011) Bioavailability of Cd in 110 polluted topsoils to recombinant bioluminescent sensor bacteria: effect of soil particulate matter. J Soil Sediment 11(2): 231–237.

Jiang W, Mashayekhi H, Xing B (2009) Bacterial toxicity comparison between nano- and micro-scaled oxide particles. Environ Pollut 157(5): 1619–1625.

Jin X, Li M, Wang J, Marambio-Jones C, Peng F, Huang X, Damoiseaux R, Hoek EMV (2010) High-throughput screening of silver nanoparticle stability and bacterial inactivation in aquatic media: influence of specific ions. Environ Sci Technol 44(19): 7321–7328.

Jones N, Ray B, Ranjit KT, Manna AC (2008) Antibacterial activity of ZnO nanoparticle suspensions on a broad spectrum of microorganisms. FEMS Microbiol Lett 279(1): 71–76.

Jung WK, Koo HC, Kim KW, Shin S, Kim SH, Park YH (2008) Antibacterial activity and mechanism of action of the silver ion on *Staphylococcus aureus* and *Escherichia coli*. Appl Environ Microbiol 74(7): 2171–2178.

Kaegi R, Ulrich A, Sinnet B, Vonbank R, Wichser A, Zuleeg S, Simmler H, Brunner S, Vonmont H, Burkhardt M, Boller M (2008) Synthetic TiO_2 nanoparticle emission from exterior facades into the aquatic environment. Environ Pollut 156(2): 233–239.

Kahru A, Dubourguier H-C (2010) From ecotoxicology to nanoecotoxicology. Toxicology 269: 105–119.

Kahru A, Savolainen K (2010) Potential hazard of nanoparticles: from properties to biological and environmental effects. Toxicol 269(2–3): 89–91.

Kahru A, Ivask A, Kasemets K, Põllumaa L, Kurvet I, François M, Dubourguier H-C (2005) Biotests and biosensors in ecotoxicological risk assessment of field soils polluted with zinc, lead and cadmium. Environ Toxicol Chem 24(11): 2973–2982.

Kahru A, Dubourguier HC, Blinova I, Ivask A, Kasemets K (2008) Biotests and biosensors for ecotoxicol of metal oxide nanoparticles: A minireview. Sensors 8(8): 5153–5170.

Käkinen A, Bondarenko O, Ivask A, Kahru A (2011) The effect of composition of different ecotoxicological test media on free and bioavailable copper from $CuSO_4$ and CuO nanoparticles: comparative evidence from a Cu-selective electrode and a Cu-biosensor. *Sensors* 11(11):10502–10521.

Kasemets K, Ivask A, Dubourguier HC, Kahru A (2009) Toxicity of nanoparticles of ZnO, CuO and TiO_2 to yeast *Saccharomyces cerevisiae*. Toxicol in Vitro 23(6): 1116–1122.

Kikuchi Y, Sunada K, Iyoda T, Hashimoto K, Fujishima A (1997) Photocatalytic bactericidal effect of TiO_2 thin films: dynamic view of the active oxygen species responsible for the effect. J Photochem Photobiol A: Chemistry 106(1–3): 51–56.

Kim JS (2007) Antibacterial activity of Ag + ion-containing silver nanoparticles prepared using the alcohol reduction method. J Ind Eng Chem 13(5): 718–722.

Kim SC, Lee DK (2005) Preparation of TiO_2-coated hollow glass beads and their application to the control of algal growth in eutrophic water. Microchem J 80(2): 227–232.

Kim JS, Kuk E, Yu KN, Kim J-H, Park SJ, Lee HJ, Kim SH, Park YK, Park YH, Hwang C-Y, Kim Y-K, Lee Y-S, Jeong DH, Cho M-H (2007) Antimicrobial effects of silver nanoparticles. Nanomed Nanotech Biol Med 3(1): 95–101.

Kim J, Jungeun L, Soonchul K, Sunghoon J (2009a) Preparation of biodegradable polymer/silver nanoparticles composite and its antibacterial efficacy. J Nanosci Nanotechnol 9: 1098–1102.

Kim KJ, Sung W, Suh B, Moon SK, Choi JS, Kim J, Lee D (2009b) Antifungal activity and mode of action of silver nano-particles on *Candida albicans*. BioMetals 22(2): 235–242.

Kimura T, Nishioka H (1997) Intracellular generation of superoxide by copper sulphate in *Escherichia coli*. Mutat Res-Gen Tox En 389(2–3): 237–242.

Kloepfer JA, Mielke RE, Nadeau JL (2005) Uptake of CdSe and CdSe/ZnS quantum dots into bacteria *via* purine-dependent mechanisms. Appl Environ Microbiol 71(5): 2548–2557.

Kvitek L, Panaček A, Soukupova J, Kolar M, Večerova R, Prucek R, Holecova M, Zboril R (2008) Effect of surfactants and polymers on stability and antibacterial activity of silver nanoparticles (NPs). J Phys Chem C 112(15): 5825–5834.

Le Pape H, Solano-Serena F, Contini P, Devillers C, Maftah A, Leprat P (2004) Involvement of reactive oxygen species in the bactericidal activity of activated carbon fibre supporting silver: bactericidal activity of ACF(Ag) mediated by ROS. J Inorg Biochem 98(6): 1054–1060.

Leskinen P, Virta M, Karp M (2003) One-step measurement of firefly luciferase activity in yeast. Yeast 20(13): 1109–1113.

Li M, Pokhrel S, Jin X, Mädler L, Damoiseaux R, Hoek EMV (2010) Stability, bioavailability, and bacterial toxicity of ZnO and iron-doped ZnO nanoparticles in aquatic media. Environ Sci Technol 45(2): 755–761.

Li M, Zhu L, Lin D (2011) Toxicity of ZnO nanoparticles to *Escherichia coli*: mechanism and the influence of medium components. Environ Sci Technol 45(5): 1977–1983.

Liau, SY, Read DC, Pugh WJ, Furr JR, Russell AD (1997) Interaction of silver nitrate with readily identifiable groups: relationship to the antibacterial action of silver ions. Lett Appl Microbiol 25: 279–283.

Liu J, Hurt, RH (2010) Ion release kinetics and particle persistence in aqueous nano-silver colloids. Environ Sci Technol 44(6): 2169–2175.

Liu Y, He L, Mustapha A, Li H, Hu ZQ, Lin M (2009) Antibacterial activities of zinc oxide nanoparticles against *Escherichia coli* O157:H7. J Appl Microbiol 107(4): 1193–1201.

Liu J, Sonshine DA, Shervani S, Hurt RH (2010) Controlled release of biologically active silver from nanosilver surfaces. ACS Nano 4(11): 6903–6913.

Lok CN, Ho CM, Chen R, He QY, Yu WY, Sun H, Tam P, Chiu JF, Che CM (2006) Proteomic analysis of the mode of antibacterial action of silver nanoparticles. J Proteome Res 5(4): 916–924.

Lok CN, Ho CM, Chen R, He QY, Yu WY, Sun H, Tam P, Chiu JF, Che CM (2007) Silver nanoparticles: partial oxidation and antibacterial activities. JBIC 12(4): 527–534.

Marambio-Jones C, Hoek EMV (2010) A review of the antibacterial effects of silver nanomaterials and potential implications for human health and the environment. JNR 12: 1531–1551.

Maynard AD (2007) Nanotechnology – toxicological issues and environmental safety and environmental safety. In: Project on Emerging Nanotechnologies, vols–14. Woodrow Wilson International Center for Scholars, Washington, DC.

McDonnell G, Russell AD (1999) Antiseptics and disinfectants: activity, action and resistance. Clin Microbiol Rev 12(1): 147–179.

Menard A, Drobne D, Jemec A (2011) Ecotoxicity of nanosized TiO_2. Review of in vivo data. Environ Pollut 159(3): 677–684.

International Council on Mining and Metals (2007) MERAG: Metals Environmental Risk Assessment Guidance. London, UK.

Midander K, Cronholm P, Karlsson HL, Elihn K, Möller L, Leygraf C, Wallinder IO (2009) Surface characteristics, copper release, and toxicity of nano- and micrometer-sized copper and copper(II) oxide particles: a cross-disciplinary study. Small 5(3): 389–399.

Morones JR, Elechiguerra JL, Camacho A, Holt KB, Kouri JB, Ramirez JT, Yacaman MJ (2005) The bactericidal effect of silver nanoparticles. Nanotechnol 16: 2346–2353.

Mortimer M, Kasemets K, Kahru A (2010) Toxicity of ZnO and CuO nanoparticles to ciliated protozoa *Tetrahymena thermophila*. Toxicol 269(2–3): 182–189.

Mueller NC, Nowack B (2008) Exposure modeling of engineered nanoparticles in the environment. Environ Sci Technol 42(12): 4447–4453.

Navarro E, Piccapietra F, Wagner B, Marconi F, Kaegi R, Odzak N, Sigg L, Behra R (2008) Toxicity of silver nanoparticles to *Chlamydomonas reinhardtii*. Environ Sci Technol 42(23): 8959–8964.

Neal A (2008) What can be inferred from bacterium–nanoparticle interactions about the potential consequences of environmental exposure to nanoparticles? Ecotoxicol 17(5): 362–371.

Nel A, Madler L, Velegol D, Xia T, Hoek EMV, Somasundaran P, Klaessig F, Castranova V, Thompson M (2009) Understanding biophysicochemical interactions at the nano-bio interface. Nat Mater 8(7): 543–557.

Niazi JH, Gu MB (2009) Toxicity of metallic nanoparticles in microorganisms - a review. In: Kim YK, Platt U, Gu MB, Iwahashi H (eds) Atmospheric and Biological Environmental Monitoring. Springer, Dordrecht/Heidelberg/London/New York.

Nowack B, Krug HF, Height M (2011) 120 years of nanosilver history: implications for policy makers. Environ Sci Technol 45(4): 1177–1183.

Pal S, Tak YK, Song JM (2007) Does the antibacterial activity of silver nanoparticles depend on the shape of the nanoparticle? A study of the gram-negative bacterium *Escherichia coli*. Appl Environ Microbiol 73(6): 1712–1720.

Panáček A, Kvítek L, Prucek R, Kolář M, Večeřová R, Pizúrová N, Sharma VK, Nevěčná TJ, Zbořil R (2006) Silver colloid nanoparticles: synthesis, characterization and their antibacterial activity. J Phys Chem B 110(33): 16248–16253.

Paquin PR, Gorsuch JW, Apte S, Batley GE, Bowles KC, Campbell PGC, Delos CG, Di Toro DM, Dwyer RL, Galvez F, Gensemer RW, Goss GG, Hogstrand C, Janssen CR, McGeer JC, Naddy RB, Playle RC, Santore RC, Schneider U, Stubblefield WA, Wood CM, Wu KB (2002) The biotic ligand model: a historical overview. Comp Biochem Physiol C 133: 3–35.

Park HJ, Kim JY, Kim J, Lee JH, Hahn JS, Gu MB, Yoon J (2009) Silver-ion-mediated reactive oxygen species generation affecting bactericidal activity. Water Res 43(4): 1027–1032.

Pesavento M, Alberti G, Biesuz R (2009) Analytical methods for determination of free metal ion concentration, labile species fraction and metal complexation capacity of environmental waters: a review. Anal Chim Acta 631(2): 129–141.

Puzyn T, Rasulev B, Gajewicz A, Hu X, Dasari TP, Michalkova A, Hwang HM, Toropov A, Leszczynska D, Leszczynski J (2011) Using nano-QSAR to predict the cytotoxicity of metal oxide nanoparticles. Nat Nano 6(3): 175–178.

Raffi M, Hussain F, Bhatti T, Akhter J, Hameed A, Hasan M (2008) Antibacterial characterization of silver nanoparticles against *E. coli* ATCC-15224. J Mater Sci Tech Ser 24: 192–196.

Rai M, Yadav A, Gade A. (2009). Silver nanoparticles as a new generation of antimicrobials. Biotechnology Advances 27(1): 76–83.

Rajendran R, Balakumar C, Mohammed Ahammed HA, Jayakumar S, Vaideki K, Rajesh EM (2010) Use of zinc oxide nano particles for production of antimicrobial textiles. Int J Eng Sci 2(1): 202–208.

Ren G, Hu D, Cheng EWC, Vargas-Reus MA, Reip P, Allaker RP (2009) Characterisation of copper oxide nanoparticles for antimicrobial applications. Int J of Antimicrob Ag 33(6): 587–590.

Rice RH, Vidrio EA, Kumfer BM, Qin Q, Willits NH, Kennedy IM, Anastasio C (2009) Generation of oxidant response to copper and iron nanoparticles and salts: stimulation by ascorbate. Chem-Biol Interact 181(3): 359–365.

Robichaud CO, Uyar AE, Darby MR, Zucker LG, Wiesner MR (2009) Estimates of upper bounds and trends in nano-TiO_2 production as a basis for exposure assessment. Environ Sci Technol 43(12): 4227–4233.

Roe D, Karandikar B, Bonn-Savage N, Gibbins B, Roullet JB (2008) Antimicrobial surface functionalization of plastic catheters by silver nanoparticles. J Antimicrob Chemother 61(4): 869–876.

Ruparelia JP, Chatterjee AK, Duttagupta SP, Mukherji S (2008) Strain specificity in antimicrobial activity of silver and copper nanoparticles. Acta Biomater 4(3): 707–716.

Sadiq IM, Dalai S, Chandrasekaran N, Mukherjee A (2011) Ecotoxicity study of titania (TiO_2) NPs on two microalgae species: *Scenedesmus sp*. and *Chlorella sp*. Ecotoxicol Environ Saf 74(5): 1180–1187.

Sambhy V, MacBride MM, Peterson BR, Sen A (2006) Silver bromide nanoparticle/polymer composites: dual action tunable antimicrobial materials. J Am Chem Soc 128(30): 9798–9808.

Sawai J (2003) Quantitative evaluation of antibacterial activities of metallic oxide powders (ZnO, MgO and CaO) by conductimetric assay. J Microbiol Meth 54(2): 177–182.

Sebastian Tomi N, Kränke B, Aberer W (2004) A silver man. Lancet 363(9408): 532.

Smetana AB, Klabunde KJ, Marchin GR, Sorensen CM (2008). Biocidal activity of nanocrystalline silver powders and particles. Langmuir 24(14): 7457–7464.

Sondi I, Salopek-Sondi B (2004) Silver nanoparticles as antimicrobial agent: a case study on *E. coli* as a model for gram-negative bacteria. J Colloid Interface Sci 275(1): 177–182.

Studer AM, Limbach LK, Van Duc L, Krumeich F, Athanassiou EK, Gerber LC, Moch H, Stark, WJ (2010) Nanoparticle cytotoxicity depends on intracellular solubility: comparison of stabilized copper metal and degradable copper oxide nanoparticles. Toxicol Lett 197(3): 169–174.

Sunada K, Kikuchi Y, Hashimoto K, Fujishima A. (1998). Bactericidal and Detoxification Effects of TiO_2 Thin Film Photocatalysts. Environmental Science & Technology 32(5):726–728.

Tayel AA, El-Tras WF, Moussa S, El-Baz AF, Mahrous H, Salem MF, Brimer L (2011) Antibacterial activity and mechanism of action of zinc oxide nanoparticles against foodborne pathogens. J Food Safety: 31(2): 211–218.

Trapalis CC, Keivanidis P, Kordas G, Zaharescu M, Crisan M, Szatvanyi A, Gartner M (2003) $TiO_2(Fe_3+)$ nanostructured thin films with antibacterial properties. Thin Solid Films 433(1–2): 186–190.

Tsuang YH, Sun JS, Huang YC, Lu CH, Chang WHS, Wang CC (2008) Studies of photokilling of bacteria using titanium dioxide nanoparticles. Artif Organs 32(2): 167–174.

Vertelov GK, Krutyakov TA, Eremenkova OV, Olenin AY, Lisichkin, GV (2008) A versatile synthesis of highly bactericidal Myramistin® stabilized silver nanoparticles Nanotechnol 19(35): 355707. doi:10.1088/0957-4484/19/35/355707.

Wei C, Lin WY, Zainal Z, Williams NE, Zhu K, Kruzic AP, Smith RL, Rajeshwar K (1994) Bactericidal activity of TiO_2 photocatalyst in aqueous media: toward a solar-assisted water disinfection system. Environ Sci Technol 28(5): 934–938.

White JML, Powell AM, Brady K, Russell-Jones R (2003) Severe generalized argyria secondary to ingestion of colloidal silver protein. Clin Exp Dermatol 28(3): 254–256.

Wu B, Huang R, Sahu M, Feng X, Biswas P, Tang YJ (2009) Bacterial responses to Cu-doped TiO_2 nanoparticles. Sci Total Environ 408(7): 1755–1758.

Wu B, Wang Y, Lee YH, Horst A, Wang Z, Chen DR, Sureshkumar R, Tang YJ (2010) Comparative eco-toxicities of nano-ZnO particles under aquatic and aerosol exposure modes. Environ Sci Technol 44(4): 1484–1489.

Xia T, Kovochich M, Liong M, Mädler L, Gilbert B, Shi H, Yeh JI, Zink JI, Nel AE (2008) Comparison of the mechanism of toxicity of zinc oxide and cerium oxide nanoparticles based on dissolution and oxidative stress properties. ACS Nano 2(10): 2121–2134.

Yoon KY, Byeon JH, Park CW, Hwang J (2008) Antimicrobial effect of silver particles on bacterial contamination of activated carbon fibers. Environ Sci Technol 42(4): 1251–1255.

Zhang L, Jiang Y, Ding Y, Povey M, York D (2007) Investigation into the antibacterial behaviour of suspensions of ZnO nanoparticles (ZnO nanofluids). JNR 9(3): 479–489.

Zhang Y, Peng H, Huang W, Zhou Y, Yan D (2008) Facile preparation and characterization of highly antimicrobial colloid Ag or Au nanoparticles. J Colloid Interface Sci 325(2): 371–376.